



Building for tomorrow: Analyzing ideal thermal transmittances in the face of climate change in Brazil

Eugénio Rodrigues^{a,*}, Jean Parente^{a,b}, Marco S. Fernandes^a

^a Univ of Coimbra, ADAI, Department of Mechanical Engineering, Rua Luís Reis Santos, Pólo II, 3030-788 Coimbra, Portugal

^b CEAU/T2P, University of Porto, Via Panorâmica Edgar Cardoso 215, 4150-564 Porto, Portugal

HIGHLIGHTS

- Ideal U -values in present-day and future climates in Brazil are determined.
- The trend of the ideal U -values varies according to each region.
- A relation between U -values and outdoor temperatures and HVAC setpoints was found.
- A fast procedure is presented to determine the trend of the ideal U -values over time.
- For each trend, building design strategies are proposed.

ARTICLE INFO

Keywords:

Climate change
Mitigation
Residential buildings
Thermal transmittance
Brazil

ABSTRACT

The climate will become hotter, and buildings will perform differently as outdoor conditions evolve. If the lowest energy demand is desired, it is crucial to determine the ideal thermophysical properties of the envelope over the buildings' life span. However, the scientific literature is still scarce in providing a compelling answer. Therefore, this study (i) determines ideal thermal transmittance values (U -values) for present-day and future climates, (ii) determines to what extent the thermophysical properties will need to change to remain ideal, (iii) identifies different trends of U -values over time, (iv) establishes a relationship between outdoor air temperatures, cooling and heating setpoints, and ideal U -values, and (v) proposes a set of design strategies according to each trend. The EPSAP generative design method was used to create a large dataset of residential buildings with random geometries and U -values to evaluate their energy demand for heating and cooling in EnergyPlus. The thermal performance of each building was evaluated for 30 locations in Brazil for the current period and two future timeframes (2050 and 2080). The Future Weather Generator tool was used to morph today's typical meteorological weather to match the EC-Earth3 data for the SSP5–8.5 scenario. Although climate change has a similar relative impact, its consequences differ over time in each location. The ideal U -values have different trends in different regions: (a) remaining unchanged in the future, (b) changing from being the highest possible to the lowest of the analyzed range in 2050 or 2080, and (c) being mid-range values in the present and with similar or lower values in the future climate. The impact on the thermal loads of maintaining the present-day ideal U -values also varies significantly in the future timeframes, from being nil to representing an increase reaching 30 % in 2050 ($\Delta 2.94 \text{ MW-h} \pm 0.06 \text{ MW-h}$) and 57 % in 2080 ($\Delta 6.05 \text{ MW-h} \pm 0.09 \text{ MW-h}$). Therefore, building design professionals need to use different strategies according to each region and consider how climate evolves during the lifetime of the building.

1. Introduction

The global building sector was responsible for 39 % of the energy and process-related carbon emissions in 2018, which have grown by 2 % for

the second consecutive year [1]. The increase in anthropogenic carbon emissions contributes to the rise of global temperatures [2] and ultimately harms human health [3].

In this sense, buildings must lower their operational energy demand

* Corresponding author.

E-mail address: erodrigues@uc.pt (E. Rodrigues).

<https://doi.org/10.1016/j.apenergy.2023.122360>

Received 24 August 2023; Received in revised form 23 October 2023; Accepted 14 November 2023

0306-2619/© 2023 The Authors. Published by Elsevier Ltd. This is an open access article under the CC BY license (<http://creativecommons.org/licenses/by/4.0/>).

[4]. For that, professionals must design high-performance buildings. However, recent studies show evidence that high-performance buildings with design variables optimized for today's environment might be at risk of underperforming in the future due to climate change [5]. As global warming progresses, environmental conditions evolve, so building designers must avoid relying only on historical climate data. This issue looms large, given its direct connection to nations' ability to meet carbon neutrality targets [6].

The pursuit of understanding whether contemporary optimized building designs will sustain their optimality in the future gives rise to several questions. Will the ideal values of building parameters exhibit variation over time? If indeed there is variation, will discernible overarching trends emerge, or will these fluctuations be regionally specific? In essence, will ideal values uniformly increase across all locations, or might they increase in one locale while concurrently decreasing in another? If distinct trends become apparent, what tailored design strategies should be formulated to address the unique characteristics of each region?

Existing research offers valuable insights into these questions, although several times contradictory. For instance, studies in North Africa and Europe indicate that certain cities along the Mediterranean coast will maintain similar ideal thermal transmittances for single-family houses [7]. Conversely, increasing insulation and using low-emissivity windows in Benevento, Italy, may paradoxically lead to worse energy performance [8]. Nevertheless, reducing heating demand will compensate for the increase in cooling needs; thus, highly insulated buildings will ensure resilience to climate change [9]. These findings illustrate the complexity of the issue and the need for tailored strategies.

Moreover, studies spanning multifamily houses in Sweden, Denmark, Germany, France, Italy, and Greece underscore the necessity of location-specific design strategies [10]. In Australia, optimized exterior wall insulation thickness, window type, and overhang depth in a typical office building will remain nearly optimized in Brisbane [5]. In contrast, the same building in Canberra will increase its cooling needs in the future [5]. In a multi-apartment building in Podgorica, Montenegro, energy demand could be reduced at the end of the century by up to 66 % if the building is highly insulated, has a lower shading operation setpoint, and employs natural ventilation [11].

Ideal parameters for building variables are undeniably dynamic and influenced by regional idiosyncrasies. In Asia, the walls' ideal thermal transmittances (U -values) in the future reached the lower bound of the studied interval on a generic multi-story building in China [12]. In Iran, the trend of ideal U -values of the building envelope was found to vary according to three regions—to be the lowest possible today and in the future for the cities on the coast of the Persian Gulf, to be lower or equal than the present values in the future in the highlands, and to be higher in the north on the coast of the Caspian Sea [13].

The scenario remains no less intricate in North America, where the significance of thermal transmittances varies based on location and building type [14]. In South America, specific challenges emerge, requiring higher U -values in Chile [15]. In Brazil, research efforts have predominantly concentrated on optimizing building designs for the present climate, with limited exploration of ideal parameters for current and future climates [16–24].

The existing literature, though valuable, is not devoid of limitations. Many studies lack a comprehensive approach and often rely on outdated climate data, hindering the derivation of definitive conclusions. This scarcity of knowledge, coupled with the absence of a unified methodology, presents an auspicious opportunity to address these gaps and provide meaningful insights.

In response to these challenges, this study thoroughly analyzes thermal transmittances within residential building envelopes across 30 distinct locations in Brazil. Employing a generative design procedure, we evaluate thousands of multi-thermal zone buildings under present-day and future climate scenarios. This comprehensive approach empowers us to determine ideal U -values for each location and climate

scenario while elucidating their trends over time.

The regions in Brazil are subsequently grouped according to their unique trends, allowing for the formulation of tailored design strategies to combat the impending impacts of climate change. Furthermore, our study introduces a novel procedure grounded in the relationship between outdoor temperatures and indoor setpoints, efficiently predicting future ideal U -values. This innovative approach facilitates determining the most suitable design strategy before embarking on the building modeling process.

In summation, this study bridges existing knowledge gaps and offers a methodology that holds potential far beyond its immediate context. It can drive sustainable and energy-efficient building design practices globally, contributing to the ongoing global effort to mitigate the impact of climate change.

2. Material and methods

This study tests the hypothesis that climate change will exert a discernible influence on the ideal thermal transmittances of single-family houses in Brazil. The anticipated outcome is to identify whether a pronounced trend in altering this thermophysical property becomes evident as global warming intensifies. By probing this hypothesis, the research strives to inform the development of context-specific design strategies tailored to each observed trend.

This work assumes dwellings to be occupied by a single family of five persons in a two-story flat-roof building on the city outskirts. A stringent climate scenario is assumed, where no further climate policies are enforced, renewable energy technological innovations are minimal, and the economy will continue to grow based on fossil fuel, leading to very high greenhouse gas emissions and, thus, leading to a significantly warmer climate. This study ignores urban context and assumes human behavior to be similar in the future. These simplifications are acceptable since (1) low-rise homes are typical in suburban areas where buildings are well-spaced with minimum shading or reflections, and (2) climate change-related tendencies are already observed nowadays.

In order to test the hypothesis, this study concept framework (Fig. 1) comprises seven steps and starts by selecting the locations over the Brazilian territory (step 1). For each location, 21st-century weather data was downloaded, and their integrity was checked (step 2). The retrieved data was used as a baseline (present-day climate) and mathematically transformed to produce future climates (step 3). In the fourth step, random geometries of single-family houses were created using a generative design method, and the thermal transmittances were randomly assigned to each building. In the fifth step, the energy demand for all buildings' air-conditioning was simulated in all scenarios and stored as datasets. In the sixth step, a preliminary analysis was carried out to group locations according to the trend of the ideal U -values over time. Lastly, the datasets were statistically analyzed, and the findings were synthesized (step 7).

2.1. Selection of locations

Brazil is a vast and diverse territory with varying regional climates. Therefore, the following criteria were used to select locations to be analyzed: (i) these should cover all climate zones found in Brazil's NBR 15220 technical norm and the greatest number of classifications found in Köppen-Geiger climate classification, (ii) these should also be distributed spatially over Brazil's latitudes with predominance for state capitals and most populated regions, (iii) these locations must have freely available hourly weather data, and (iv) the historical meteorological data must match the baseline period of the weather morphing tool.

Brazil presently has seven climate types according to the Köppen-Geiger classification. Fig. 2 depicts two maps of Brazil for the present-day (1980–2016 timeframe) and future (2071–2100 timeframe, RCP8.5 scenario) climates at 1-km resolution according to this

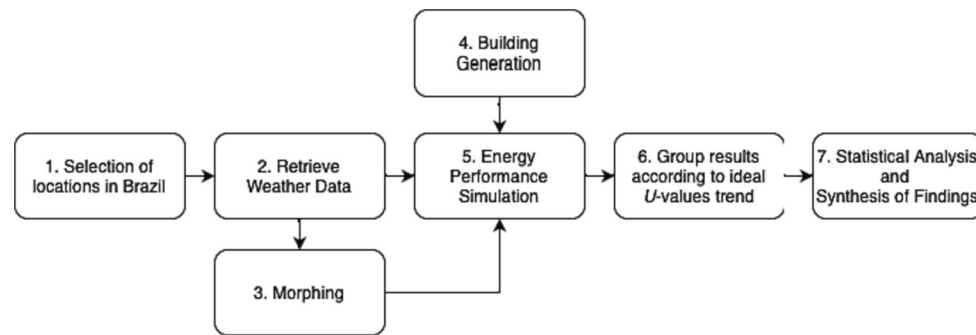


Fig. 1. Study concept framework.

classification [25]. In the future, we can observe an increase in the dry arid steppe (BSh) and desertic (BWh) areas on the northeast, a reduction in tropical wet areas (Af) on the northwest, and a fading of dry winter and wet summer areas (Cwa and Cwb) and humid subtropical areas (Cfa and Cfb) on the south of the country. A warmer and dryer future climate leads to a larger tropical savannah area (Aw) on Brazil's mainland.

The selection phase involved 30 locations covering several populated areas, different latitudes, altitudes, and climate types. For example, Manaus, Salvador, and Santos are tropical rainforest (Af), Petrolina is hot arid steppe (Bsh), Curitiba and Caxias do Sul are temperate without dry season (Cfb), Franca is temperate with dry winter and hot summer (Cwa), and Poços de Caldas is temperate with dry winter and warm summer (Cwb). All remaining locations are tropical savannah (Aw). From all, 12 locations will change to a different climate classification, such as Manaus and São Paulo (Am), Salvador, Franca, São Carlos, Campinas, and Maringá (Aw), Mossoró and Vitória da Conquista (BSh), Curitiba and Caxias do Sul (Cfa), and Poços de Caldas (Cwa). Table 1 depicts the geographical and climate information for all locations.

2.2. Weather morphing

In order to have the most representative results for the present-day climate, 21st-century hourly weather data for each location was retrieved from the climate.onebuilding.org website [26]. The weather data is provided in EnergyPlus Weather Format, following the TMY/ISO 15927-4:2005 methodology, and derived from meteorological records between 2004 and 2018.

The future weather data is obtained by morphing the present-day weather to match a projected climate change scenario in two timeframes (2050 and 2080). The procedure statistically shifts and stretches the present-day weather data [27]. The 'shift' ($x = x_0 + \Delta x_m$) adds the monthly change (Δx_m) to the present-day variable (x_0). The 'stretch' ($x = \alpha_m \cdot x_0$) scales the present-day variable (x_0) by multiplying it by the fraction of the monthly change (α_m). Lastly, when 'shift' and 'stretch' are combined, $x = x_0 + \Delta x_m + \alpha_m(x - x_0)$, the mean and variance of the present-day variable, or just the variance, are adjusted.

In this study, the data is morphed using the Future Weather Generator [28], which employs climate data from the EC-Earth3 model used in the CMIP6 experiments [29] (which served as a basis for the 6th IPCC Assessment Report published in 2022). The EC-Earth3 validation may be found in Refs. [30, 31]. Although the tool implements four Shared Socioeconomic Pathways (SSP), this study only considers SSP5–8.5, being one of the IPCC's scenarios [32], which projects an $8.5 \text{ W}\cdot\text{m}^{-2}$ of radiative forcing. Although some researchers argue that SSP5–8.5 is unpalatable [33], others consider its study the highest priority due to its projected consequences [34]. This scenario projects current CO_2 emissions doubling by 2050 and the average global temperature rising 4.3°C by 2100. Monthly changes are computed from each median month of the present-day period (1985–2014) and the two future timeframes—2050 (2036–2065) and 2080 (2066–2095). The tool's world grid has a

nominal resolution of 100 km, and the variables' monthly changes are spatially downscaled using a bilinear interpolation method of the four nearest points of the grid to the weather data's location.

The formulation is fully described on the documentation page of the tool's website [35].

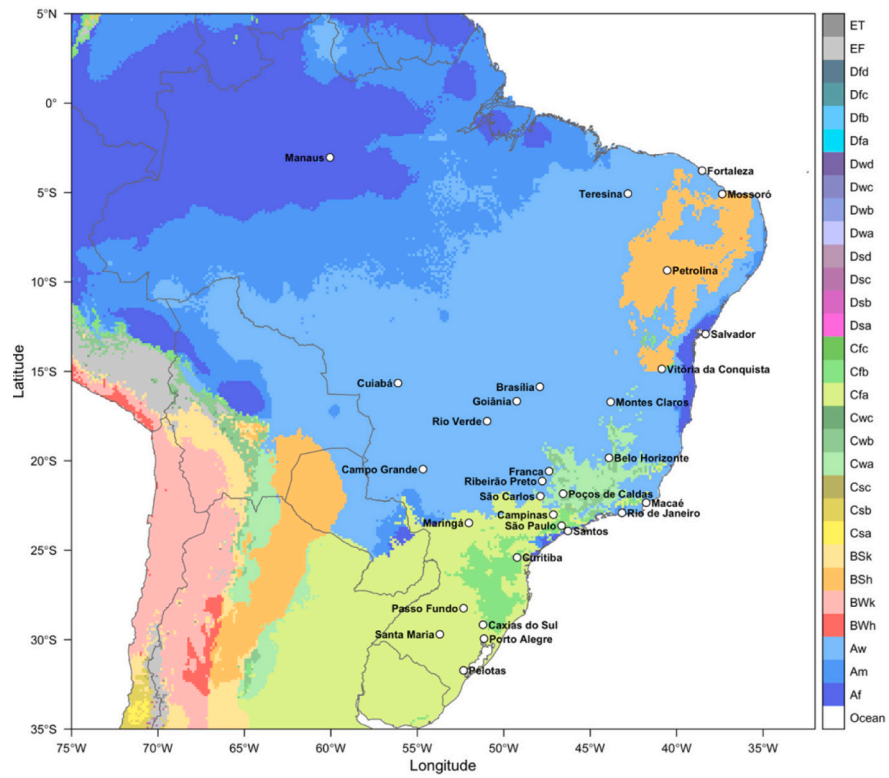
2.3. Building geometry generation

The dataset of building geometries is created using the EPSAP algorithm [36]. The algorithm produces alternative geometries by determining the indoor space arrangement of a given functional program by satisfying all specifications. The generative algorithm is a hybrid evolution strategy approach. The traditional mutation operator is replaced by a stochastic hill climbing method that performs geometric actions, such as translation, rotation, stretching, and mirroring of an element, room, cluster of rooms, stories, and the whole layout. The EPSAP algorithm minimizes a weighted-sum cost function of seventeen penalty functions that evaluate (i) the building's maximum gross and construction areas, compactness, and circulation areas, (ii) the zones' overflow, connectivity, overlapping, fixed position, dimensions, and relative importance, and (iii) the openings' accessibility, dimensions, overlap, orientation, and fixed position.

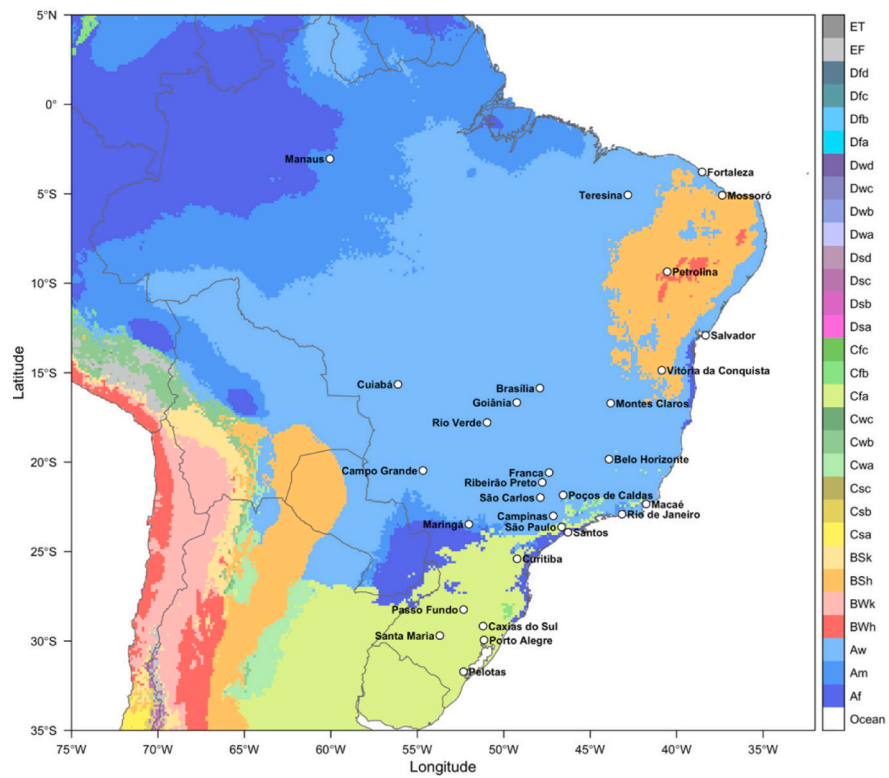
The algorithm starts by generating a random population of alternative designs in the evolution strategy stage. Then, each design is transformed in the stochastic hill climbing stage to minimize the cost function. When no further improvements are possible, the algorithm returns to the evolution strategy stage, where half of the population with the worst fitness is eliminated and replaced by new randomly generated designs. This process continues cyclically until the evolution strategy stage can no longer improve the fitness of the elite individuals—i.e., the number of alternative designs chosen by the user, which is a small part of the entire population. Further details on the EPSAP algorithm may be found in Ref. [37, 38] and its validation in Ref. [39].

The building specifications correspond to a two-story family house (see Table 2). The ground floor comprises a hall, a living room, a kitchen, and a bathroom, and on the second floor, a corridor connects two double bedrooms, a single bedroom, and a second bathroom. A staircase serves both levels. The geometry specifications for each zone include type (circulation, service, or living), relative importance (ranks the importance of each zone in comparison to the remaining zones from none to max), associated stories, minimum zone floor side dimension, minimum zone floor area, and ratios for the zone floor sides. The geometry specifications for the exterior openings are type (door, gate, or window), minimum width, minimum height, and relative vertical position of the opening to the story floor level. Relatively to the interior openings, the adjacency relations of contiguous zones are also specified.

Fig. 3 displays 24 examples of building geometries, showing diversity in orientation, indoor arrangements, and building shapes. Although exterior windows are the same size, the window-to-wall and window-to-floor ratios vary among buildings, as these are only required to satisfy each room's minimum dimensions and areas. A large dataset of building



(a) Present-day climate (1980-2016).



(b) Future climate (RCP8.5, 2071-2100).

Fig. 2. Map of Brazil and its current and future climate classification [25].

Table 1

Geographic data and climate classification (sorted in descending latitude) [25]. Future climate classification that differs from the present-day climate is marked in bold.

City	Location			-	Climate		
	Lat.	Long.	Alt. (m)		Present-day	Present-day description	Future *
Manaus	3.04° S	60.05° W	81	Af	Tropical, rainforest	Am	
Fortaleza (coastal)	3.78° S	38.53° W	25	Aw	Tropical, savannah	Aw	
Teresina	5.06° S	42.82° W	67	Aw	Tropical, savannah	Aw	
Mossoró (coastal)	5.08° S	37.37° W	38	Aw	Tropical, savannah	BSh	
Petrolina	9.35° S	40.55° W	385	BSh	Arid, steppe, hot	BSh	
Salvador (coastal)	12.91° S	38.33° W	20	Af	Tropical, rainforest	Aw	
Vitória da Conquista	14.86° S	40.86° W	914	Aw	Tropical, savannah	BSh	
Cuiabá	15.65° S	56.12° W	188	Aw	Tropical, savannah	Aw	
Brasília	15.86° S	47.91° W	1060	Aw	Tropical, savannah	Aw	
Goiânia	16.67° S	49.25° W	772	Aw	Tropical, savannah	Aw	
Montes Claros	16.71° S	43.82° W	648	Aw	Tropical, savannah	Aw	
Rio Verde	17.79° S	50.96° W	784	Aw	Tropical, savannah	Aw	
Belo Horizonte	19.83° S	43.92° W	827	Aw	Tropical, savannah	Aw	
Campo Grande	20.47° S	54.67° W	559	Aw	Tropical, savannah	Aw	
Franca	20.58° S	47.38° W	1028	Cwa	Temperate, dry winter, hot summer	Aw	
Ribeirão Preto	21.13° S	47.77° W	549	Aw	Tropical, savannah	Aw	
Poços de Caldas	21.84° S	46.57° W	1260	Cwb	Temperate, dry winter, warm summer	Cwa	
São Carlos	21.98° S	47.88° W	865	Cfa	Temperate, no dry season, hot summer	Aw	
Macaé (coastal)	22.34° S	41.77° W	2	Aw	Tropical, savannah	Aw	
Rio de Janeiro (coastal)	22.91° S	43.16° W	3	Aw	Tropical, savannah	Aw	
Campinas	23.01° S	47.14° W	661	Cfa	Temperate, no dry season, hot summer	Aw	
Maringá	23.48° S	52.02° W	545	Cfa	Temperate, no dry season, hot summer	Aw	
São Paulo	23.63° S	46.66° W	802	Cfa	Temperate, no dry season, hot summer	Am	
Santos (coastal)	23.93° S	46.29° W	3	Af	Tropical, rainforest	Af	
Curitiba	25.41° S	49.23° W	932	Cfb	Temperate, no dry season, warm summer	Cfa	
Passo Fundo	28.24° S	52.33° W	724	Cfa	Temperate, no dry season, hot summer	Cfa	
Caxias do Sul	29.17° S	51.20° W	759	Cfb	Temperate, no dry season, warm summer	Cfa	
Santa Maria	29.70° S	53.70° W	95	Cfa	Temperate, no dry season, hot summer	Cfa	
Porto Alegre (coastal)	29.95° S	51.14° W	8	Cfa	Temperate, no dry season, hot summer	Cfa	
Pelotas (coastal)	31.72° S	52.33° W	18	Cfa	Temperate, no dry season, hot summer	Cfa	

* Projected climate classification under RCP8.5 scenario and 2071–2100 timeframe [25].

Table 2

Geometry and topological specifications for zones and openings. Based on Rodrigues & Fernandes [7].

Zone	C ^{sn}	C ^{sf}	C ^{ri}	C ^{sl}	C ^{su}	C ^{ss} (m)	C ^{sa} (m ²)	C ^{ssr} (-)	C ^{slr} (-)
S ₁	Hall	Circulation	Min	L ₁	L ₁	2.70	10.0	{2.0, 3.0}	{3.0, 1.5}
S ₂	Living room	Living	Max	L ₁	L ₁	3.20	-	1.7	2.0
S ₃	Kitchen	Service	Mid	L ₁	L ₁	1.80	-	1.7	2.0
S ₄	Bathroom	Service	Min	L ₁	L ₁	2.20	-	1.7	2.0
S ₅	Stair	Circulation	-	L ₁	L ₂	-	-	-	-
S ₆	Corridor	Circulation	None	L ₂	L ₂	1.40	6.0	{2.0, 3.0}	{3.0, 1.5}
S ₇	Double bedroom	Living	High	L ₂	L ₂	2.70	-	1.7	2.0
S ₈	Double bedroom	Living	High	L ₂	L ₂	2.70	-	1.7	2.0
S ₉	Single bedroom	Living	Mid	L ₂	L ₂	2.70	-	1.7	2.0
S ₁₀	Bathroom	Service	Min	L ₂	L ₂	2.20	-	1.7	2.0

C^{sn} – name, C^{sf} – function, C^{ri} – relative importance, C^{sl} and C^{su} – served lower and upper stories, C^{ss} – minimum side, C^{sa} – minimum area, C^{ssr} and C^{slr} – zone smaller and larger side ratios, L₁ and L₂ – story 1 and 2.

Exterior Opening	C ^{os}	C ^{oet}	C ^{oew} (m)	C ^{oeh} (m)	C ^{oew} (m)	Interior Opening	C ^{oit}	C ^{oia}	C ^{oib}	C ^{oiw} (m)	C ^{oih} (m)	C ^{oiv} (m)
Oe ₁	S ₁	Door	1.00	2.00	0	Oi ₁	Door	S ₁	S ₂	0.90	2.00	0
Oe ₂	S ₂	Window	2.80	2.00	0	Oi ₂	Door	S ₁	S ₃	0.90	2.00	0
Oe ₃	S ₃	Window	1.20	1.00	1.00	Oi ₃	Door	S ₁	S ₄	0.90	2.00	0
Oe ₄	S ₄	Window	0.60	0.60	1.40	Oi ₄	Door	S ₅	S ₁	0.90	2.00	0
Oe ₅	S ₅	Window	0.80	1.40	0.80	Oi ₅	Adj.	S ₂	S ₃	0	-	-
-	S ₆	-	-	-	-	Oi ₆	Door	S ₅	S ₆	0.90	2.00	0
Oe ₆	S ₇	Window	1.80	1.00	1.00	Oi ₇	Door	S ₆	S ₇	0.90	2.00	0
Oe ₇	S ₈	Window	1.80	1.00	1.00	Oi ₈	Door	S ₆	S ₈	0.90	2.00	0
Oe ₈	S ₉	Window	1.20	1.00	1.00	Oi ₉	Door	S ₆	S ₉	0.90	2.00	0
-	S ₁₀	-	-	-	-	Oi ₁₀	Door	S ₆	S ₁₀	0.90	2.00	0

C^{os} – zone, C^{oet} – opening type, C^{oew} – width, C^{oeh} – height, C^{oew} – vertical position, C^{oit} – type, C^{oia} and C^{oib} – connecting zones, C^{oiw} – width, C^{oih} – height, C^{oiv} – vertical position, Adj. – adjacency.

geometries allows us to reduce the implicit bias that a single building may produce and analyze the statistical distribution of its energy performance. Therefore, the results will be more robust.

2.4. Building performance simulation

For each geometry in the generated dataset, the building's energy performance was evaluated using EnergyPlus after the EPSAP algorithm concluded the building generation process [40]. Each building model

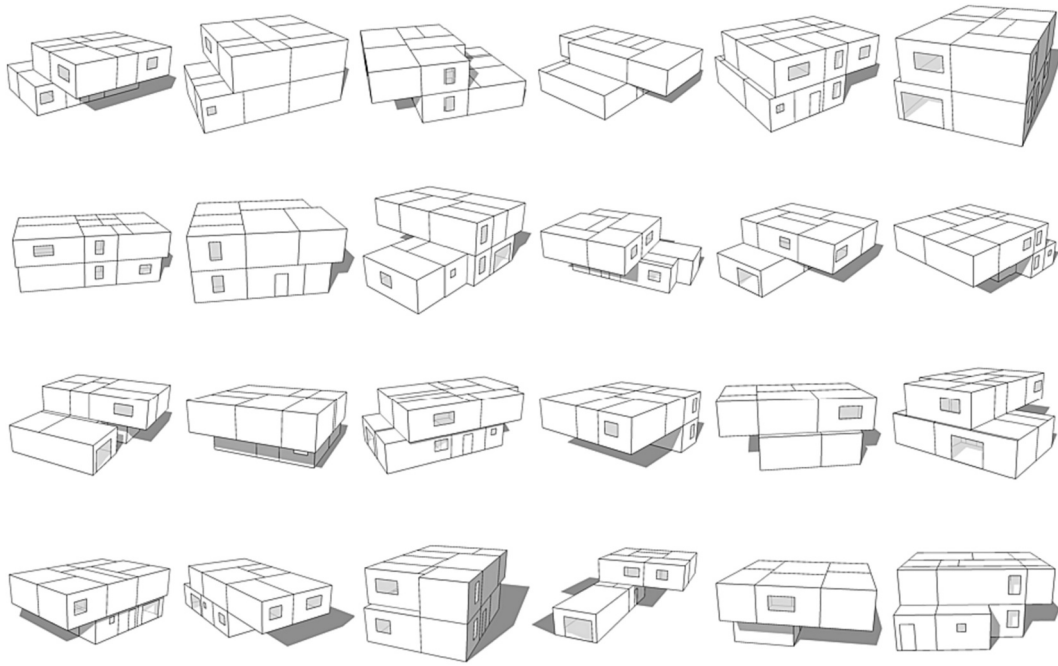


Fig. 3. Examples of the EPSAP-generated building geometries.

consisted of ten thermal zones, one per room in the building geometry specifications.

The selected time step for each simulation was 15 min. The solar distribution was considered full exterior with reflections, and the shadow calculation was carried out by the polygon clipping algorithm with simple sky diffuse modeling. The adaptive convection algorithm and TARP were used for the outside and inside surface convection algorithms, respectively. The heat balance was determined using the conduction transfer function. The outputs were related to the thermal energy demand of the building—i.e., the total, heating, and cooling energy needs.

The internal gains, HVAC, and construction specifications are described in the following sections.

2.4.1. Internal gains specifications

The specifications for internal gains (occupancy, lighting, and equipment) are presented in Fig. 4 and Table 3 and correspond to a typified single-family house of five dwellers. The lighting and equipment design levels and schedules are based on the building’s zone type and occupancy. Furthermore, daylighting controls dim the light intensity in zones with exterior windows, switching them off when daylight illuminance exceeds 300 lx. This dimming control is a ‘simulation

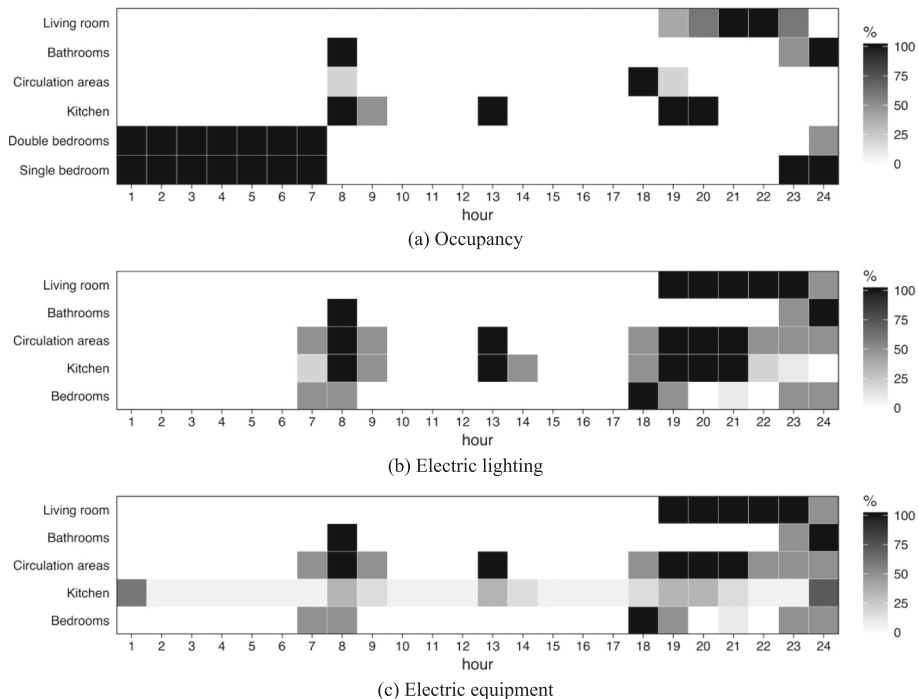


Fig. 4. Internal gains use pattern in each zone. From Rodrigues & Fernandes [7].

Table 3
Internal gains specifications in each zone. Based on Rodrigues & Fernandes [7].

Zone type	Occupancy		Electric lighting	Electric equipment
	Max. number of people *	Activity level (W·person ⁻¹)	Design level (W·m ⁻²)	Design level (W)
Living room	5	110	7.5	350
Bathrooms	1	207	7.5	100
Circulation areas	1	190	3.2	20
Kitchen	2	190	5.0	1440
Double bedrooms	2	72	7.5	250
Single bedroom	1	72	7.5	250

* Number of dwellers accessing each zone and not necessarily the number of occupants simultaneously in the zone. The occupants' distribution is defined together with the proper occupancy schedules.

procedure' to adjust the lighting values according to the available daylight in each latitude since the electric lighting profiles are identical in all locations. The window shadings are closed during nighttime.

2.4.2. HVAC and airflow specifications

Cooling and heating are only considered in the living room and the bedrooms due to being occupied for long periods. The HVAC template zone ideal loads air system model is used, with the heating and cooling availability schedule defined by the zone's occupancy pattern. This "ideal" system was employed since it allows us to evaluate and report each zone's thermal needs directly. The setpoints of the temperature thermostat for cooling and heating are 25 °C and 20 °C, respectively, which fall within the dead band proposed in ASHRAE Standard 55–2017. Air exhaust is considered in the kitchen and bathrooms with 0.6 air changes per hour and occurring during occupancy defined for these zones. In all zones, 0.4 or 0.2 air changes per hour (zones with or without exterior openings, respectively) are considered for outdoor air infiltration. Although the passive house standard is 0.6 air changes per hour [41], several research studies point to lower values in existing buildings [42,43]. In our study, the selected values represent an airtight building, allowing us to focus on the thermal impact of the envelope's physical properties. As we determine the energy loads for heating and cooling, we do not consider natural ventilation, as this can be one of the strategies to release excessive indoor heat.

Table 4
Thermophysical properties of the building elements. Based on Rodrigues & Fernandes [7].

Element	Layer	Thick. (m)	k (W·m ⁻¹ ·K ⁻¹)	ρ (kg·m ⁻³)	c_p (J·kg ⁻¹ ·K ⁻¹)	U (W·m ⁻² ·K ⁻¹)	Mass (kg·m ⁻²)	SHGC (–)	
Ground floor	Structural layer	0.200	1.730	2245.6	836.8	0.437	509.69	–	
	Insulation layer	0.080	0.040	32.1	836.8				
	Filling layer	0.020	0.800	1600.0	840.0				
	Regulation layer	0.010	0.220	950.0	840.0				
	Finishing layer	0.020	0.200	825.0	2385.0				
Interior door	Finishing layer	0.005	0.200	825.0	2385.0	2.009	21.15	–	
	Structural layer	0.030	0.067	430.0	1260.0				
	Finishing layer	0.005	0.200	825.0	2385.0				
Interior wall	Finishing layer	0.020	0.220	950.0	840.0	4.499	195.01	–	
	Structural layer	0.070	1.730	2243.0	836.8				
	Finishing layer	0.020	0.220	950.0	840.0				
Interior slab	Finishing layer	0.020	0.220	950.0	840.0	2.841	494.12	–	
	Structural layer	0.200	1.730	2245.6	836.8				
	Regulation layer	0.010	0.220	950.0	840.0				
	Finishing layer	0.020	0.200	825.0	2385.0				
	Opaque (exterior wall, roof, and suspended floor)	Thermal mass is equivalent to the mass of the interior slab.							RAND {0.05, ..., 1.25}
Transparent (window)	–					RAND {0.2, ..., 5.0}		–	0.6

k – thermal conductivity, ρ – density, c_p – specific heat, U – thermal transmittance, SHGC – solar heat gain coefficient.

2.4.3. Construction specifications

The thermophysical properties of the construction elements are presented in Table 4. The thermal mass of exterior walls, roofs, and suspended floors is equivalent to that of the interior slab and the element's surface area. The thermal, solar, and visible absorptances are 0.9, 0.75, and 0.75, respectively. Their U -value is assigned before the dynamic simulations randomly between 0.05 W·m⁻²·K⁻¹ and 1.25 W·m⁻²·K⁻¹ in steps of 0.05 W·m⁻²·K⁻¹. Overall, the building presents a high thermal mass. The ground floor is in contact with the soil at a constant temperature of 18 °C in all months. Regarding the transparent elements, their U -value is proportionally paired with one of the opaque elements and ranges between 0.2 W·m⁻²·K⁻¹ and 5.0 W·m⁻²·K⁻¹ in steps of 0.2 W·m⁻²·K⁻¹. The pairing of U -values follows the tendency of real cases, where the U -values' of both opaque and transparent elements decrease or increase proportionally.

2.5. Comparison analysis and synthesis

The final synthetic dataset was created with the buildings' geometry, construction, and performance data for each location with the present-day and the 2050 and 2080 timeframes. With these datasets, a graph comparison and statistical analysis were conducted by splitting each dataset into groups according to the thermal transmittance values of their envelope elements. The total energy demand for heating and cooling, the standard deviation, and the differences in total, cooling, and heating energy needs between the present-day and the 2050 and 2080 timeframes were calculated. The buildings with the lowest total thermal energy needs—optimum energy performance—define the ideal U -values for transparent and opaque elements. Knowing the ideal U -values for the present-day and future timeframes makes it possible to determine if today's ideal U -values will be the same in the future and, if not, how much will contribute to the building energy demand for heating and cooling.

3. Results

The present-day weather data were downloaded from the climate.onebuilding.org website for all these locations and morphed according to the SSP5–8.5 scenario (2050 and 2080 timeframes). The present-day weather followed the typical meteorological year methodology derived from historical records between 2004 and 2018, except for Mossoró, Caxias do Sul, and São Paulo, which were from historical records ranging between 2007 and 2021. The results of the morphing process and the comparison of each environmental variable to the present-day values are presented and discussed individually in each group section

below. In addition, each location is also classified according to its altitude—ranging from sea level (or coastal), < 300 m, > 300 m, > 500 m, > 700 m, and > 900 m—to better understand why some cities belong to a specific group.

The results of the energy performance assessment were preliminarily analyzed to group the locations according to their ideal U -values trend in the future, which led to four groups. Fig. 5 depicts the map of locations by group. Group 1 (red dots) corresponds to locations where the ideal U -values in the present day are the lowest of the thermal transmittance range and will be the same in the future. Groups 2 (green squares) and 3 (blue triangles) depict the extreme changes in ideal U -values, locations having high ideal values in present-day climate and very low ideal values in the future. The difference between the two groups is presenting or not such extreme change in 2050. Lastly, Group 4 (black diamonds) includes all remaining locations that show ideal U -values that tend to be lower or equal in the future climate. The results of each group are presented and discussed in the subsections below.

3.1. Group 1

The first group comprises cities between southern parallels 3° and 17° , distributed throughout the States of Amazonas, Mato Grosso, Goiás, Bahia, Pernambuco, Rio Grande do Norte, and Ceará. These cities have altitudes below 300 m, except for Goiânia, which has an altitude between 700 m and 900 m. From those cities below 300 m, Fortaleza, Mossoró, and Salvador are coastal at sea level.

Considering the most impactful environmental variables for the building's thermal performance in this group (Table 5), dry-bulb temperature and global horizontal radiation will rise. At the same time,

relative humidity will decrease. This trend is found in the remaining groups as well. The annual average dry-bulb temperatures in present-day climate range between 25°C and 29°C , and the minimum and maximum dry-bulb temperatures reach 21°C and 35°C , respectively. Dry-bulb temperatures will increase by around 2.8°C and 5.3°C in 2050 and 2080, respectively. Global horizontal radiation in present-day climate varies between $213\text{ W}\cdot\text{h}\cdot\text{m}^{-2}$ and $262\text{ W}\cdot\text{h}\cdot\text{m}^{-2}$, and it will rise $5.3\text{ W}\cdot\text{h}\cdot\text{m}^{-2}$ and $7.7\text{ W}\cdot\text{h}\cdot\text{m}^{-2}$ in 2050 and 2080 timeframes, respectively. As temperature rises, relative humidity, whose annual average varies between 55 % and 80 %, will decrease, reaching -6% in 2050 and -13% in 2080. Wind speeds will not have meaningful changes in the locations from Group 1 and any locations from the other groups. The results show that global warming will particularly impact all locations from all groups, as the temperature rise is higher than the global average temperature increase expected in the SPP5–8.5 scenario.

Fig. 6 depicts the energy demand for today and future climates for each step of the buildings' thermal transmittance variation (x -axis). The graphs in the first column depict the total and cooling energy demand for present-day (green line), 2050 (orange line), and 2080 (red line) timeframes—the black circumference indicates the ideal U -values, which is the one with the lowest energy demand. The blue line indicates the cooling demand for each timeframe (when the total and cooling demands are equal, the blue line is covered by the total energy demand line). The second column illustrates the graphs with standard deviation (σ) for each step of U -values. The third and fourth columns depict total energy (black bars), cooling (blue bars), and heating (red bars) demand differences (Δ) between 2050 and present-day climates—minimum and maximum difference percentages are indicated in the corresponding bars.

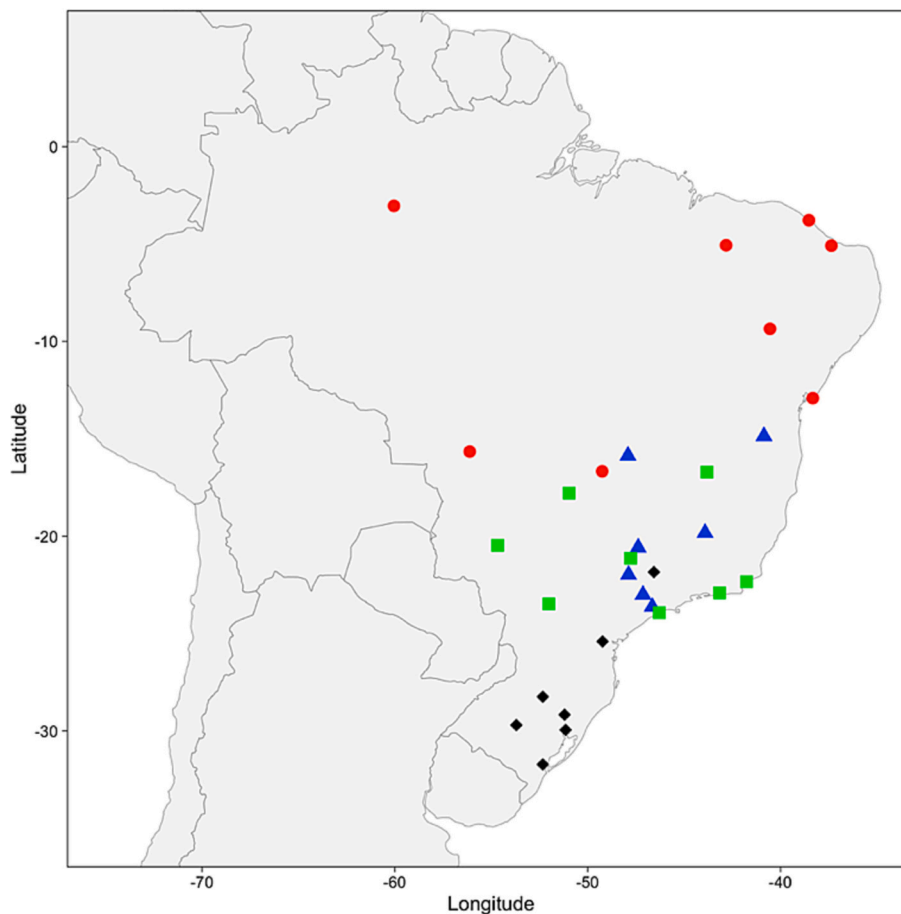


Fig. 5. Locations grouped by the trend of the ideal U -values. Red dots depict Group 1, green squares Group 2, blue triangles Group 3, and black diamonds Group 4. (For interpretation of the references to colour in this figure legend, the reader is referred to the web version of this article.)

Table 5

Group 1 – Dry-bulb temperature, relative humidity, global horizontal radiation, and wind speed variables comparison between present-day and 2050 and 2080 timeframes (hourly average and present-day to timeframe difference).

Location	Timeframe	Dry-bulb temperature				Relative humidity		Global horizontal radiation		Wind speed	
		°C	Δ °C	Min °C	Max °C	%	Δ %	W·h·m ⁻²	Δ W·h·m ⁻²	m·s ⁻¹	Δ m·s ⁻¹
Manaus (< 300 m)	Present-day	26.6		23.2	31.5	80.0		213.2		1.4	
	2050	29.3	2.7	25.9	34.2	73.7	-6.4	218.1	4.8	1.4	0
	2080	31.9	5.3	28.6	36.8	67.3	-12.8	220.5	7.3	1.5	0.1
Fortaleza (coastal)	Present-day	27.2		24.7	30.2	73.8		258.1		5.2	
	2050	29.9	2.7	27.5	32.9	68.0	-5.8	263.1	5.1	5.3	0.1
	2080	32.5	5.3	30.1	35.5	62.3	-11.5	265.6	7.5	5.5	0.3
Teresina (< 300 m)	Present-day	29.1		24.5	34.8	69.1		258.2		1.8	
	2050	31.9	2.8	27.2	37.5	63.7	-5.4	263.4	5.2	1.8	0
	2080	34.5	5.3	29.9	40.0	58.4	-10.6	265.8	7.6	1.8	0.1
Mossoró (coastal)	Present-day	27.6		23.7	32.2	71.2		244.7		3.5	
	2050	30.3	2.8	26.4	34.9	65.6	-5.6	249.9	5.2	3.5	0
	2080	32.9	5.3	29.1	37.5	60.3	-10.9	252.3	7.6	3.7	0.2
Petrolina (> 300 m)	Present-day	27.7		22.5	33.6	55.1		262.0		3.9	
	2050	30.4	2.8	25.3	36.4	51.7	-3.5	267.3	5.3	3.9	0
	2080	33.0	5.3	27.9	38.9	48.1	-7.0	269.7	7.7	4.1	0.2
Salvador (coastal)	Present-day	26.5		23.9	28.9	76.4		240.5		4.4	
	2050	29.2	2.8	26.8	31.7	70.0	-6.4	245.8	5.3	4.5	0.1
	2080	31.8	5.3	29.4	34.2	64.3	-12.1	248.2	7.7	4.7	0.2
Cuiabá (< 300 m)	Present-day	26.5		21.8	32.5	68.6		225.0		2.4	
	2050	29.2	2.8	24.6	35.2	63.9	-4.7	230.3	5.3	2.5	0
	2080	31.8	5.3	27.2	37.7	59.2	-9.3	232.7	7.7	2.6	0.1
Goiânia (> 700 m)	Present-day	25.4		21.2	30.4	59.9		236.7		1.4	
	2050	28.2	2.8	24.0	33.1	56.6	-3.3	242.0	5.3	1.5	0
	2080	30.7	5.3	26.6	35.6	52.9	-7.1	244.4	7.7	1.5	0.1

According to the first column in Fig. 6, a line pattern emerges, showing that energy demand will increase in the whole range of U -values as the climate evolves toward 2050 and 2080. A steady decrease in energy demand is observable in each timeframe as U -values also reduce. Therefore, the minimum demand is found for the lowest U -values possible—except Goiânia, for which the ideal U -values are slightly above the lowest possible ones. In addition, for all these locations, the total energy demand is characterized alone by cooling needs in all timeframes. For the lowest U -values, these cooling demands present an increase of 17 % to 22 % in 2050 concerning the present timeframe, versus a 35 % to 54 % increase for the highest U -values, as depicted in the last column in Fig. 6, benefiting the lowest ideal thermal transmittances observed in Group 1. Moreover, since the energy needs comprise only cooling demands, the same results are observed for the total energy demand increment between the referred timeframes (third column in Fig. 6).

As U -values decrease, the energy demand difference between present-day and future timeframes reduces, showing that low thermal transmittances raise the robustness of buildings. This effect is also confirmed when looking at the buildings' energy demand standard deviation, depicted in the second-column graphs in Fig. 6. As the U -values reduce, standard deviation also diminishes in all timeframes, showing that geometry becomes less relevant in affecting the building performance. Nonetheless, as the climate gets warmer in the future, standard deviation increases in the whole range of U -values, particularly for high U -values. Therefore, low U -values make the buildings' performance similar in different timeframes and make their geometry less relevant.

Goiânia is of particular interest. In this location, the buildings' energy demand in the present-day climate is practically constant throughout the range of U -values, meaning that no meaningful performance difference is found in having the lowest or the highest thermal transmittances. However, a slightly higher standard deviation is verified for higher U -values. When looking at the outdoor dry-bulb temperatures, we notice that the average minimum temperature is 21 °C and the average temperature is 25 °C, which fall within the setpoints of the operation of the HVAC system. This location defines the departure from Group 1 ideal U -values trend to the one in Group 2 presented below.

In order to understand the impact of today's ideal U -values under a future climate, it is important to compare it with the future ideal U -

values in different timeframes. The ideal U -values in this group are the same for all timeframes; thus, no difference is observed. As stated, the only one that differs is Goiânia, which has present-day U -values of 0.1 W·m⁻²·K⁻¹ for opaque elements and 0.4 W·m⁻²·K⁻¹ for transparent elements (Table 6). Although a small difference, those present ideal U -values, if maintained in the future, correspond to a 5 % increase in cooling needs (0.5 MW·h \pm 0.08 MW·h) in 2050 and a 3% in 2080 (0.4 MW·h \pm 0.08 MW·h), in comparison with the future ideal U -values.

3.2. Group 2

In the case of Group 2, the cities are found between the southern parallels 16° and 24°. These locations are distributed over the States of Minas Gerais, Goiás, Mato Grosso do Sul, Rio de Janeiro, Paraná, and São Paulo. Rio Verde has an altitude between 700 m and 900 m, Monte Carlos, Campo Grande, Ribeirão Preto, and Maringá are found between 500 m and 700 m, and Macaé, Rio de Janeiro, and Santos are coastal cities at sea level.

In this group, the annual average dry-bulb temperatures in present-day climate are slightly lower than in Group 1, ranging between 22 °C and 24 °C (Table 7). Similarly, the minimum and maximum dry-bulb temperatures reach 17 °C and 31 °C, respectively. Although the temperatures are lower than in Group 1, the future increase in dry-bulb temperatures is similar in both timeframes. This temperature increase is found in all groups. Global horizontal radiation in present-day climate varies between 192 W·h·m⁻² and 240 W·h·m⁻², being slightly lower than in Group 1, and it will rise the same amount as in Group 1 for both timeframes. Relative humidity, whose annual average varies between 63 % and 82 %, will reach -6 % in 2050 and -11 % in 2080.

As outdoor temperatures get slightly colder, the line pattern of energy demand found in the previous Group 1 shifts in Group 2, especially in the present-day climate. As stated for Group 1, Goiânia marked the transition between an ideal U -values trend of the lowest possible in the present-day toward higher values in the future. Fig. 7 depicts the impact of such a transition, with dramatic consequences. In the present-day climate, as U -values increase, the energy demand decreases steadily, defining a downward line pattern. However, as the present-day outdoor dry-bulb temperatures in Group 2 are colder than in Group 1 (25 °C to 29 °C versus 22 °C to 24 °C average temperatures), as climate warms up,

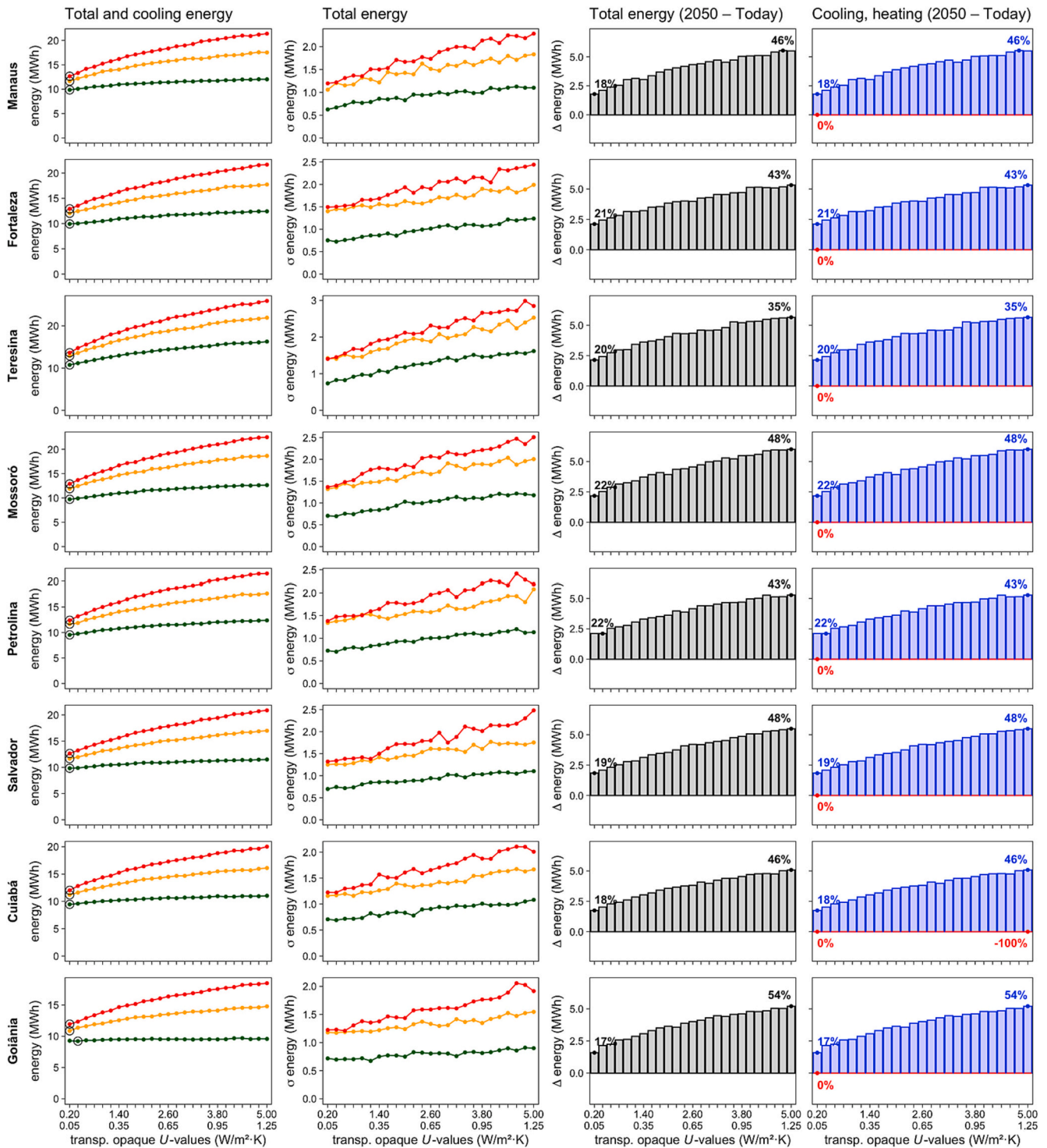


Fig. 6. Group 1– Comparison between present-day (green lines), 2050 (orange), and 2080 (red) timeframes. Graphs in the first column depict the average total energy needs – blue lines illustrate cooling energy needs, and black circles indicate the ideal pair of U -values for each timeframe. The second column presents the standard deviation (σ). The third and fourth columns present the difference in total energy needs (Δ) and cooling (blue bars) and heating (red bars) energy needs (Δ) between the 2050 and present-day timeframes. (For interpretation of the references to colour in this figure legend, the reader is referred to the web version of this article.)

future timeframes will show the same pattern found in Group 1. Thus, the present-day climate ideal U -values are the highest or near the highest value possible, while future ideal U -values will be the lowest possible in 2050 and 2080.

Another difference is that, in a few locations, geometry has less influence on the energy demand in the higher range of U -values, which is

the opposite of what is observed in Group 1 and the remaining locations in Group 2. Montes Claros, Campo Grande, Maringá, and Santos show a pattern of buildings' geometry with a lower standard deviation in the energy demand for buildings with higher thermal transmittances in the present-day climate (second column of graphs in Fig. 7). Montes Claros is even more extreme, showing the same pattern in 2050 and 2080. This

Table 6Group 1 – Overheating from the present-day ideal U -values in future timeframes (impacts greater or equal to 3% are marked in bold).

Location	Present-day ideal U -values	2050				2080			
		Ideal U -values		Impact of present-day ideal U -values		Ideal U -values		Impact of present-day ideal U -values	
		Energy (MW·h)	Δ energy (MW·h)	Δ energy (%)	ΔU -values* ($W\cdot m^{-2}\cdot K^{-1}$)	Energy (MW·h)	Δ energy (MW·h)	Δ energy (%)	ΔU -values* ($W\cdot m^{-2}\cdot K^{-1}$)
Manaus (< 300 m)	0.05/0.2	11.64 ±	0 ± 0.07	–	–	12.66 ±	0 ± 0.08	–	–
		1.06				1.20			
Fortaleza (coastal)	0.05/0.2	12.04 ±	0 ± 0.09	–	–	12.91 ±	0 ± 0.09	–	–
		1.40				1.50			
Teresina (< 300 m)	0.05/0.2	12.89 ±	0 ± 0.09	–	–	13.64 ±	0 ± 0.09	–	–
		1.42				1.40			
Mossoró (coastal)	0.05/0.2	11.89 ±	0 ± 0.09	–	–	12.89 ±	0 ± 0.09	–	–
		1.32				1.37			
Petrolina (> 300 m)	0.05/0.2	11.65 ±	0 ± 0.09	–	–	12.40 ±	0 ± 0.09	–	–
		1.34				1.38			
Salvador (coastal)	0.05/0.2	11.66 ±	0 ± 0.08	–	–	12.64 ±	0 ± 0.08	–	–
		1.25				1.32			
Cuiabá (< 300 m)	0.05/0.2	11.20 ±	0 ± 0.08	–	–	12.03 ±	0 ± 0.08	–	–
		1.16				1.22			
Goiânia (> 700 m)	0.10/0.4	11.38 ±	0.51 ± 0.08	5	–0.05/–0.2	12.34 ±	0.40 ± 0.08	3	–0.05/–0.2
		1.17				1.23			

* Opaque and transparent elements' delta U -values, respectively, for the difference between present-day and future ideal U -values.**Table 7**

Group 2 – Dry-bulb temperature, relative humidity, global horizontal radiation, and wind speed variables comparison between present-day and 2050 and 2080 timeframes (hourly average and present-day to timeframe difference).

Location	Timeframe	Dry-bulb temperature				Relative humidity		Global horizontal radiation		Wind speed	
		°C	Δ °C	Min °C	Max °C	%	Δ %	$W\cdot h\cdot m^{-2}$	$\Delta W\cdot h\cdot m^{-2}$	$m\cdot s^{-1}$	$\Delta m\cdot s^{-1}$
Montes Claros (> 500 m)	Present-day	23.9		18.3	30.2	62.8		240.1		2.0	
	2050	26.6	2.8	21.0	32.9	59.3	–5.7	245.4	5.3	2.0	0
	2080	29.2	5.3	23.6	35.4	55.4	–11.2	247.8	7.7	2.1	0.1
Rio Verde (> 700 m)	Present-day	23.7		19.7	28.5	67.2		231.3		1.7	
	2050	26.5	2.8	22.4	31.2	63.2	–3.6	236.5	5.3	1.7	0
	2080	29.1	5.3	25.1	33.7	59.0	–7.6	238.9	7.7	1.7	0.1
Campo Grande (> 500 m)	Present-day	24.0		19.2	29.8	65.9		228.9		4.4	
	2050	26.7	2.8	21.9	32.5	61.9	–4.2	234.2	5.3	4.5	0
	2080	29.3	5.3	24.6	35.0	57.8	–8.7	236.6	7.7	4.7	0.1
Ribeirão Preto (> 500 m)	Present-day	23.9		18.1	30.8	69.6		219.6		2.4	
	2050	26.6	2.8	20.9	33.6	65.2	–3.1	224.9	5.3	2.4	0
	2080	29.2	5.3	23.5	36.1	60.6	–6.7	227.3	7.7	2.5	0.1
Macaé (coastal)	Present-day	24.1		19.9	30.1	78.8		216.0		3.0	
	2050	26.9	2.8	22.7	32.8	72.9	–4.3	221.3	5.3	3.0	0
	2080	29.4	5.3	25.3	35.3	67.3	–8.9	223.7	7.7	3.2	0.1
Rio de Janeiro (coastal)	Present-day	24.3		21.5	28.0	78.0		206.0		3.0	
	2050	27.1	2.8	24.3	30.7	71.8	–4.2	211.4	5.3	3.1	0
	2080	29.6	5.3	26.9	33.2	66.2	–8.7	213.8	7.7	3.2	0.2
Maringá (> 500 m)	Present-day	22.6		17.8	27.9	72.9		216.2		3.7	
	2050	25.3	2.8	20.6	30.7	68.3	–4.2	221.5	5.3	3.7	0
	2080	27.9	5.3	23.3	33.2	63.6	–8.6	223.9	7.7	3.9	0.2
Santos (coastal)	Present-day	22.1		17.4	26.9	82.1		191.5		2.0	
	2050	24.9	2.8	20.2	29.6	76.0	–5.7	196.8	5.3	2.0	0
	2080	27.4	5.3	22.8	32.1	70.2	–11.2	199.2	7.7	2.0	0.1

extreme pattern will also be seen in Group 3 and Group 4 locations.

Another similarity to Group 1 is that Group 2 presents almost no heating needs, and in the cases that might have, these are almost absent in 2050 (third and fourth columns of graphs in Fig. 7). Maringá is the only location in 2050 with a residual 5 % heating need compared with the present-day climate. Lastly, and almost similarly, Maringá and Santos display a near-flatten energy demand in the 2050 timeframe, as observed in Goiânia in the present-day climate (Group 1).

As in Group 1, for the lowest U -values, the cooling demands present a smaller increase in 2050 concerning the present timeframe (12 % to 35 %) than for the highest U -values (59 % to 85 %). However, since the ideal thermal transmittance values for both timeframes are found in the two extremes of the spectrum, the cooling demand increase results in an intermediate value. Regarding the total energy demand, these are exclusively, or almost exclusively, comprised of cooling needs and,

therefore, the same increments are observed—with a slight exception in Maringá due to the minor heat demand.

The fact that present-day ideal U -values are in the opposite range of future ideal ones has a significant impact on building design in the locations of this group, as the design strategy should be very different to reach optimum energy performances. Table 8 shows the energy demand differences regarding the use of present-day ideal U -values in future timeframes. In 2050, the energy difference varies between 9 % (0.75 MW·h ± 0.05 MW·h) in Santos and 30 % (2.94 MW·h ± 0.06 MW·h) in Rio de Janeiro. In 2080, it reaches even higher energy differences. For example, Santos will present 33 % more energy demand (3.29 MW·h ± 0.06 MW·h) and Rio de Janeiro 57 % (6.05 MW·h ± 0.09 MW·h).

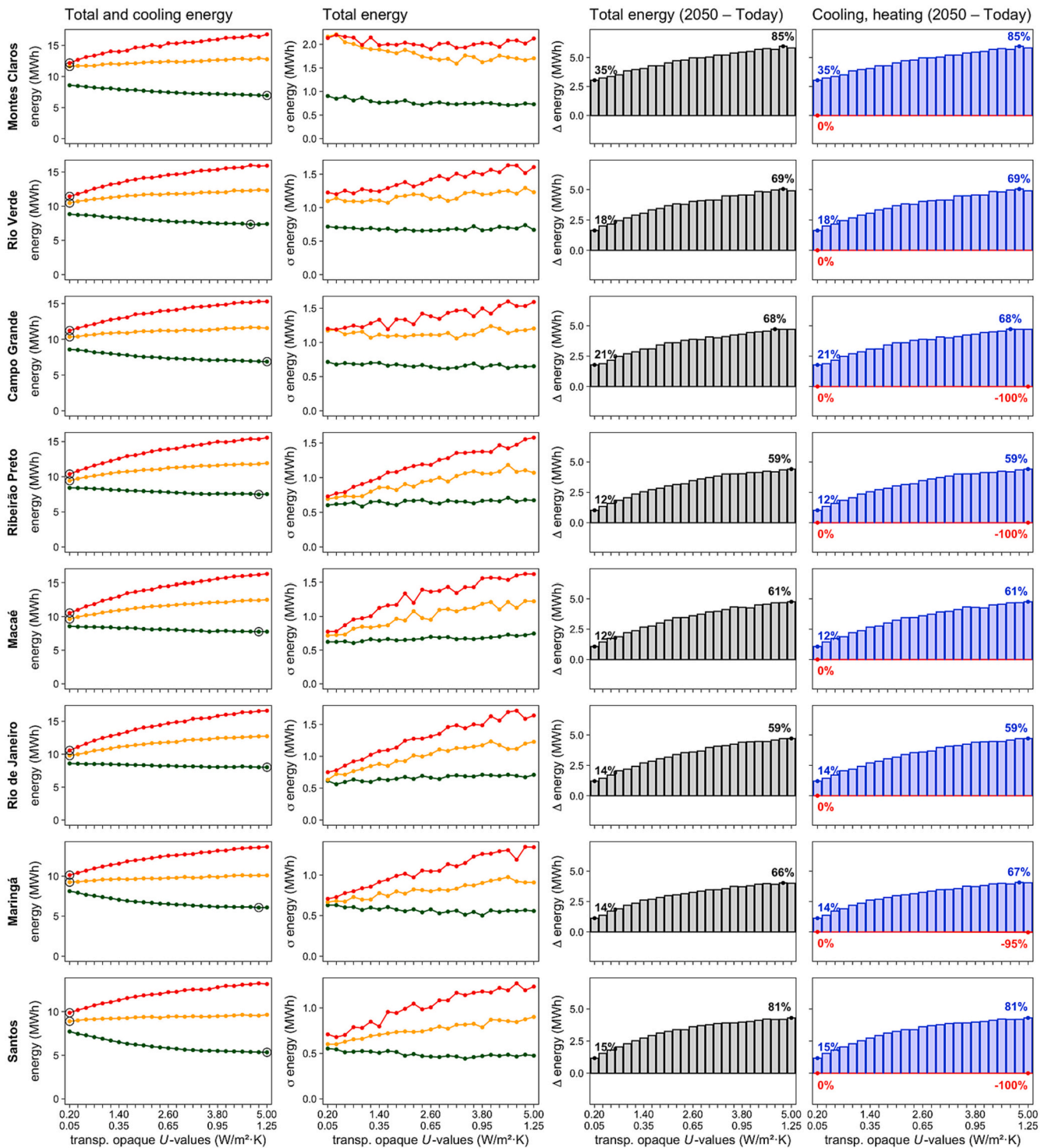


Fig. 7. Group 2 – Comparison between present-day (green lines), 2050 (orange), and 2080 (red) timeframes. Graphs in the first column depict the average total energy needs – blue lines illustrate cooling energy needs, and black circles indicate the ideal pair of U-values for each timeframe. The second column presents the standard deviation (σ). The third and fourth columns present the difference in total energy needs (Δ) and cooling (blue bars) and heating (red bars) energy needs (Δ) between the 2050 and present-day timeframes. (For interpretation of the references to colour in this figure legend, the reader is referred to the web version of this article.)

3.3. Group 3

The locations from Group 3 are placed between the southern parallels 14° and 24°, distributed over the States of Bahia, Minas Gerais, São Paulo, and Brasília Federal District. The cities of Vitória da Conquista, Brasília, and Franca have altitudes above 900 m, and Belo Horizonte,

São Carlos, and São Paulo are found between 700 m and 900 m. Lastly, Campinas is between 500 m and 700 m.

Relatively to the environmental variables in this group (Table 9), the annual average dry-bulb temperatures in present-day climate range between 20 °C and 22 °C, and the minimum and maximum dry-bulb temperatures reach 17 °C and 28 °C, respectively. Again, the increase

Table 8Group 2 – Overheating from the present-day ideal U -values in future timeframes (impacts greater or equal to 3% are marked in bold).

Location	Present-day ideal U -values	2050				2080			
		Ideal U -values		Impact of present-day ideal U -values		Ideal U -values		Impact of present-day ideal U -values	
		Energy (MW-h)	Δ energy (MW-h)	Δ energy (%)	ΔU -values* ($W\cdot m^{-2}\cdot K^{-1}$)	Energy (MW-h)	Δ energy (MW-h)	Δ energy (%)	ΔU -values* ($W\cdot m^{-2}\cdot K^{-1}$)
Montes Claros (> 500 m)	1.25/5.0	12.78 ± 1.70	1.15 ± 0.12	10	−1.20/−4.8	16.79 ± 2.12	4.62 ± 0.14	38	−1.20/−4.8
Rio Verde (> 700 m)	1.15/4.6	12.29 ± 1.21	1.82 ± 0.08	17	−1.10/−4.4	15.99 ± 1.63	4.55 ± 0.09	40	−1.10/−4.4
Campo Grande (> 500 m)	1.25/5.0	11.57 ± 1.20	1.23 ± 0.08	12	−1.20/−4.8	15.29 ± 1.59	4.08 ± 0.09	36	−1.20/−4.8
Ribeirão Preto (> 500 m)	1.20/4.8	11.82 ± 1.11	2.39 ± 0.06	25	−1.15/−4.6	15.35 ± 1.55	4.98 ± 0.08	48	−1.15/−4.6
Macaé (coastal)	1.20/4.8	12.44 ± 1.23	2.79 ± 0.07	29	−1.15/−4.6	16.16 ± 1.62	5.61 ± 0.08	53	−1.15/−4.6
Rio de Janeiro (coastal)	1.25/5.0	12.74 ± 1.23	2.94 ± 0.06	30	−1.20/−4.8	16.63 ± 1.64	6.05 ± 0.09	57	−1.20/−4.8
Maringá (> 500 m)	1.20/4.8	10.10 ± 0.91	0.85 ± 0.05	9	−1.15/−4.6	13.58 ± 1.35	3.46 ± 0.07	34	−1.15/−4.6
Santos (coastal)	1.25/5.0	9.64 ± 0.90	0.75 ± 0.05	9	−1.20/−4.8	13.16 ± 1.23	3.29 ± 0.06	33	−1.20/−4.8

* Opaque and transparent elements' delta U -values, respectively, for the difference between present-day and future ideal U -values.**Table 9**

Group 3 – Dry-bulb temperature, relative humidity, global horizontal radiation, and wind speed variables comparison between present-day and 2050 and 2080 timeframes (hourly average and present-day to timeframe difference).

Location	Timeframe	Dry-bulb temperature				Relative humidity		Global horizontal radiation		Wind speed	
		°C	Δ °C	Min °C	Max °C	%	Δ %	$W\cdot h\cdot m^{-2}$	$\Delta W\cdot h\cdot m^{-2}$	$m\cdot s^{-1}$	$\Delta m\cdot s^{-1}$
Vitória da Conquista (> 900 m)	Present-day	21.0		16.9	26.2	78.9		234.3		3.4	
	2050	23.7	2.8	19.7	28.9	73.2	−5.7	239.6	5.3	3.4	0
	2080	26.3	5.3	22.3	31.4	67.7	−11.2	242.0	7.7	3.5	0.1
Brasília (> 900 m)	Present-day	21.8		16.5	27.6	65.1		231.7		2.4	
	2050	24.5	2.8	19.3	30.3	61.5	−3.6	237.0	5.3	2.4	0
	2080	27.1	5.3	21.9	32.8	57.5	−7.6	239.4	7.7	2.5	0.1
Belo Horizonte (> 700 m)	Present-day	20.9		16.8	25.7	71.3		226.7		2.8	
	2050	23.7	2.8	19.6	28.5	67.1	−4.2	232.0	5.3	2.8	0
	2080	26.2	5.3	22.2	31.0	62.6	−8.7	234.4	7.7	2.9	0.1
Franca (> 900 m)	Present-day	21.8		18.1	26.0	63.6		235.2		2.1	
	2050	24.6	2.8	20.9	28.8	60.6	−3.1	240.5	5.3	2.1	0
	2080	27.1	5.3	23.5	31.3	56.9	−6.7	242.9	7.7	2.1	0.1
São Carlos (> 700 m)	Present-day	21.3		17.2	26.1	71.5		233.7		2.4	
	2050	24.1	2.8	20.0	28.8	67.1	−4.3	239.0	5.3	2.4	0
	2080	26.7	5.3	22.6	31.4	62.6	−8.9	241.4	7.7	2.5	0.1
Campinas (> 500 m)	Present-day	21.5		16.8	27.2	70.8		220.4		4.1	
	2050	24.2	2.8	19.6	30.0	66.5	−4.2	225.7	5.3	4.1	0
	2080	26.8	5.3	22.2	32.5	62.0	−8.7	228.2	7.7	4.3	0.2
São Paulo (> 700 m)	Present-day	20.4		16.9	25.3	71.0		192.5		3.3	
	2050	23.1	2.8	19.7	28.1	66.7	−4.2	197.8	5.3	3.4	0
	2080	25.7	5.3	22.3	30.6	62.3	−8.6	200.2	7.7	3.5	0.2

in dry-bulb temperatures will be 2.8 °C and 5.3 °C in the 2050 and 2080 timeframes, respectively. Global horizontal radiation in present-day climate varies between 193 $W\cdot h\cdot m^{-2}$ and 235 $W\cdot h\cdot m^{-2}$, and it will rise 5.3 $W\cdot h\cdot m^{-2}$ and 7.7 $W\cdot h\cdot m^{-2}$ in the 2050 and 2080 timeframes, respectively. Relative humidity, whose annual average varies between 64% and 79% in the present day, will reach −6% in 2050 and −11% in 2080.

Although placed in the same Brazilian territory as the ones in Group 2, the cities from Group 3 are colder in present-day climate (average dry-bulb temperatures from 20 °C to 22 °C *versus* 22 °C to 24 °C) due to most being in higher altitudes. Therefore, not only are the ideal U -values in the present-day the highest possible, but the same tendency is observed in the 2050 timeframe; however, not in 2080, which presents the lowest U -values. Fig. 8 illustrates this pattern. Vitória da Conquista, Brasília, Belo Horizonte, Franca, and São Paulo all have the highest or near the highest U -values in 2050. São Carlos and Campinas are transitioning,

showing an almost flat energy demand pattern in 2050, thus having an intermediate thermal transmittance value.

Similarly, in the 2080 timeframe, São Paulo also presents a flattened energy demand line but still has the lowest possible ideal U -value. As in Group 2, the locations in this group are characterized as almost not having heating needs in the present-day climate, and when they exist, these will mostly disappear in 2050. As in the previous groups, for the lowest U -values, the cooling needs exhibit a smaller increase in 2050 compared to the current timeframe (13% to 36%) than for the highest U -values (84% to 176%), as shown in the last column in Fig. 8. Thus, since the current and 2050 ideal U -values in Group 3 correspond to the highest ones, the cooling demand increases more than for the ideal cases in Groups 1 and 2. This pattern is also observed for the total energy requirements (third column in Fig. 8).

Relatively to the influence of the buildings' geometry, the second column from Fig. 8 shows a more pronounced pattern of having less

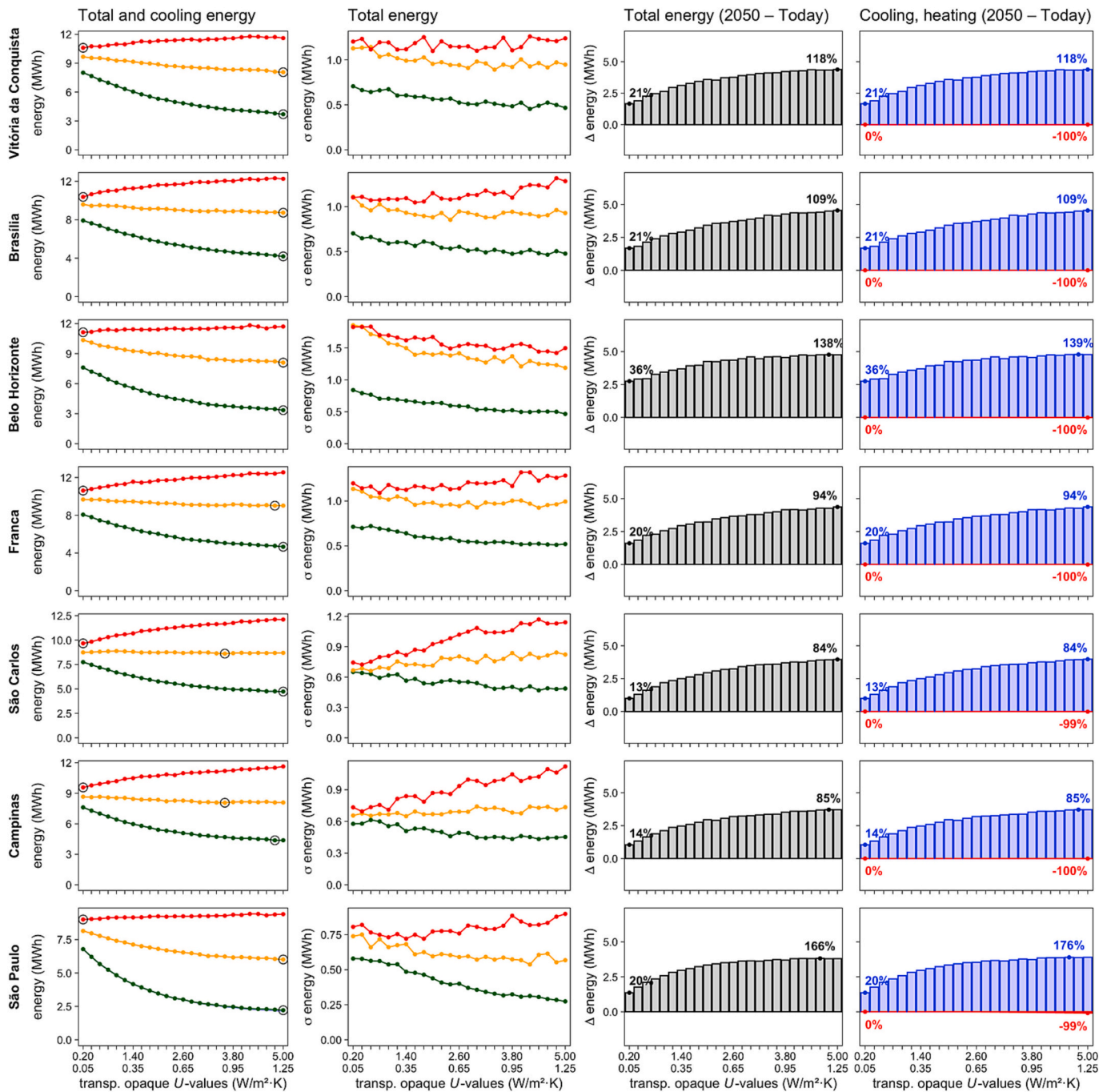


Fig. 8. Group 3 – Comparison between present-day (green lines), 2050 (orange), and 2080 (red) timeframes. Graphs in the first column depict the average total energy needs – blue lines illustrate cooling energy needs, and black circles indicate the ideal pair of U -values for each timeframe. The second column presents the standard deviation (σ). The third and fourth columns present the difference in total energy needs (Δ) and cooling (blue bars) and heating (red bars) energy needs (Δ) between the 2050 and present-day timeframes. (For interpretation of the references to colour in this figure legend, the reader is referred to the web version of this article.)

influence on the energy demand as thermal transmittances increase. This pattern is observed for all cities in the present-day climate, for Vitória da Conquista, Brasília, Belo Horizonte, Franca, and São Paulo in the 2050 timeframe, and for Belo Horizonte in the 2080 timeframe.

When analyzing the impact of the present-day ideal U -values in future timeframes, Table 10 shows that most locations have the same values in 2050. In the ones that do not, the energy demand difference is equal to or smaller than 1 % (Franca, São Carlos, and Campinas). However, in the 2080 timeframe, the values vary between 4 % ($0.4 \text{ MW}\cdot\text{h} \pm 0.06 \text{ MW}\cdot\text{h}$) and 25 % ($2.44 \text{ MW}\cdot\text{h} \pm 0.06 \text{ MW}\cdot\text{h}$) increase in

energy demand.

3.4. Group 4

In Group 4, the cities are distributed between the southern parallels 21° and 32° in the States of Minas Gerais, Paraná, Santa Catarina, and Rio Grande do Sul. Poços de Caldas and Curitiba have altitudes above 900 m, Passo Fundo and Caxias do Sul between 700 m and 900 m, and Santa Maria, Porto Alegre, and Pelotas are at sea level. Both Porto Alegre and Pelotas are coastal cities.

Table 10

Group 3 – Overheating from the present-day ideal U -values in future timeframes (impacts greater or equal to 3% are marked in bold).

Location	Present-day ideal U -values	2050				2080			
		Ideal U -values		Impact of present-day ideal U -values		Ideal U -values		Impact of present-day ideal U -values	
		Energy (MW·h)	Δ energy (MW·h)	Δ energy (%)	ΔU -values* ($W\cdot m^{-2}\cdot K^{-1}$)	Energy (MW·h)	Δ energy (MW·h)	Δ energy (%)	ΔU -values* ($W\cdot m^{-2}\cdot K^{-1}$)
Vitória da Conquista (> 900 m)	1.25/5.0	8.07 ± 0.95	0 ± 0.06	–	–	11.61 ± 1.24	1.01 ± 0.08	10	–1.20/–4.8
Brasília (> 900 m)	1.25/5.0	8.74 ± 0.93	0 ± 0.06	–	–	12.26 ± 1.28	1.89 ± 0.08	18	–1.20/–4.8
Belo Horizonte (> 700 m)	1.25/5.0	8.10 ± 1.19	0 ± 0.06	–	–	11.71 ± 1.50	0.57 ± 0.11	5	–1.20/–4.8
Franca (> 900 m)	1.25/5.0	9.02 ± 0.99	< 0.01 ± 0.06	< 1	–0.05/–0.2	12.55 ± 1.28	1.93 ± 0.08	18	–1.20/–4.8
São Carlos (> 700 m)	1.25/5.0	8.69 ± 0.82	0.08 ± 0.05	1	–0.35/–1.4	12.11 ± 1.14	2.44 ± 0.06	25	–1.20/–4.8
Campinas (> 500 m)	1.20/4.8	8.09 ± 0.71	0.02 ± 0.05	< 1	–0.30/–1.2	11.50 ± 1.06	1.93 ± 0.06	20	–1.15/–4.6
São Paulo (> 700 m)	1.25/5.0	6.01 ± 0.57	0 ± 0.05	–	–	9.41 ± 0.90	0.40 ± 0.06	4	–1.20/–4.8

* Opaque and transparent elements' delta U -values, respectively, for the difference between present-day and future ideal U -values.

Relatively to the environmental variables in this group (Table 11), the annual average dry-bulb temperatures in present-day climate range between 17 °C and 19 °C, and the minimum and maximum dry-bulb temperatures reach 9 °C and 27 °C, respectively. Global horizontal radiation in present-day climate varies between 176 $W\cdot h\cdot m^{-2}$ and 210 $W\cdot h\cdot m^{-2}$. The rise in temperatures and global horizontal radiation are similar to the ones found in previous groups. Relative humidity, whose annual average varies between 74 % and 83 %, will decrease by a maximum of 5 % in 2050 and 11 % in 2080.

When analyzing the energy demand, Fig. 9 shows that buildings in Group 4 have a distinct behavior compared to the ones in previous groups in all timeframes. As outdoor dry-bulb temperatures in this group are significantly lower than in Group 3 (average dry-bulb temperatures in present-day vary from 17 °C to 19 °C versus 20 °C to 22 °C), and subsequently than in Groups 1 and 2, even if temperatures rise 5 °C in the 2080 timeframe, the ideal U -values will not be the lowest possible.

In the first column in Fig. 9, the energy demand presents an inverted curvilinear pattern where the lowest energy demand is found in the

middle and highest thermal transmittances for most cases. Nonetheless, the ideal U -values trend over time differs among cities. In Poços de Caldas, Santa Maria, and Porto Alegre, the trend is to have lower ideal U -values in the future, while in Curitiba, Passo Fundo, Caxias do Sul, and Pelotas, the trend is to have similar values among timeframes.

Of all groups, Group 4 is the only one to present significant heating needs in the present day, with a few in 2050 and almost none in 2080. Again, for the lowest U -values, the cooling demands present a smaller increase in 2050 compared to the present timeframe (17 % to 24 %) than for the highest U -values (82 % to 219 %), as seen in the last column in Fig. 9. However, a 64 % to 84 % heating demand decrease is observed for the highest U -values, while low thermal transmittances do not exhibit heating needs in any timeframe. These variances in both heating and cooling demands combine to maximum increase values of total energy needs between both timeframes all across the U -values range (e.g., 65 % increase for a high U -value in Poços de Caldas, and 84 % for a low U -value in Caxias do Sul), according to the third column in Fig. 9. Furthermore, since there are no heating demands for low thermal

Table 11

Group 4 – Dry-bulb temperature, relative humidity, global horizontal radiation, and wind speed variables comparison between present-day and 2050 and 2080 timeframes (hourly average and present-day to timeframe difference).

Location	Timeframe	Dry-bulb temperature				Relative humidity		Global horizontal radiation		Wind speed	
		°C	Δ °C	Min °C	Max °C	%	Δ %	$W\cdot h\cdot m^{-2}$	$\Delta W\cdot h\cdot m^{-2}$	$m\cdot s^{-1}$	$\Delta m\cdot s^{-1}$
Poços de Caldas (> 900 m)	Present-day	17.7		9.4	26.8	83.0		204.9		2.2	
	2050	20.5	2.8	12.2	29.6	77.9	–5.1	210.2	5.3	2.2	0
	2080	23.0	5.3	14.9	32.1	72.3	–10.7	212.6	7.7	2.3	0.1
Curitiba (> 900 m)	Present-day	17.6		13.6	22.6	82.6		175.9		2.8	
	2050	20.4	2.8	16.4	25.4	77.5	–5.1	181.2	5.3	2.8	0
	2080	23.0	5.3	19.0	27.9	72.2	–10.4	183.6	7.7	2.9	0.2
Passo Fundo (> 700 m)	Present-day	18.0		12.9	23.2	74.1		210.0		3.8	
	2050	20.7	2.8	15.7	25.9	70.5	–3.7	215.3	5.3	3.8	0
	2080	23.3	5.3	18.3	28.4	66.2	–7.9	217.7	7.7	3.9	0.2
Caxias do Sul (> 700 m)	Present-day	16.9		12.4	22.2	82.3		190.6		2.7	
	2050	19.7	2.8	15.2	24.9	77.9	–4.3	195.9	5.3	2.8	0
	2080	22.3	5.3	17.8	27.4	73.0	–9.3	198.3	7.7	2.9	0.1
Santa Maria (sea level)	Present-day	18.4		12.1	24.5	81.9		203.7		1.7	
	2050	21.2	2.8	14.9	27.3	77.3	–4.6	209.0	5.3	1.7	0
	2080	23.7	5.3	17.5	29.8	72.1	–9.8	211.3	7.7	1.7	0.1
Porto Alegre (coastal)	Present-day	19.3		14.3	24.9	78.8		187.6		2.9	
	2050	22.1	2.8	17.1	27.7	74.8	–4.0	192.8	5.3	3.0	0
	2080	24.7	5.3	19.7	30.2	70.2	–8.6	195.3	7.7	3.1	0.1
Pelotas (coastal)	Present-day	18.7		13.1	24.1	80.3		181.1		3.6	
	2050	21.5	2.8	15.9	26.8	75.7	–4.6	186.4	5.3	3.7	0
	2080	24.0	5.3	18.6	29.4	70.9	–9.4	188.8	7.7	3.8	0.2

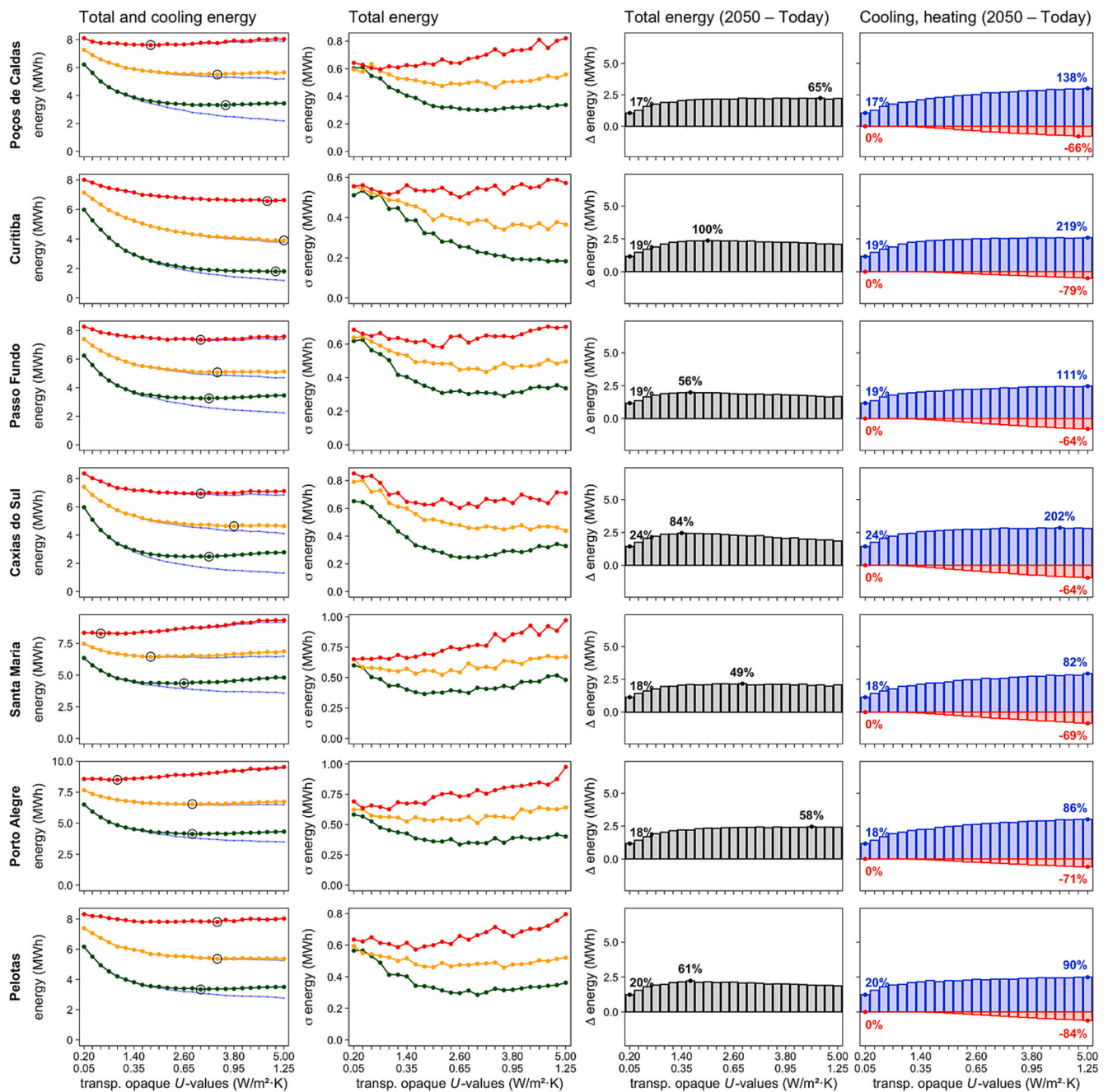


Fig. 9. Group 4 – Comparison between present-day (green lines), 2050 (orange), and 2080 (red) timeframes. Graphs in the first column depict the average total energy needs – blue lines illustrate cooling energy needs, and black circles indicate the ideal pair of U -values for each timeframe. The second column presents the standard deviation (σ). The third and fourth columns present the difference in total energy needs (Δ) and cooling (blue bars) and heating (red bars) energy needs (Δ) between the 2050 and present-day timeframes. (For interpretation of the references to colour in this figure legend, the reader is referred to the web version of this article.)

transmittances, the minimum increase values of total energy needs are observed for the lowest U -values (17 % to 24 %). This group has no clear pattern for the energy demands variation of the ideal U -values' cases.

Another interesting result is the influence of building geometry (second column of graphs in Fig. 9). Contrary to other groups, the cities in this group show that in the lowest and highest ranges of thermal transmittance, the building geometry is more impactful in the energy demand for almost all timeframes and locations. In warmer future climates, building geometry has a stronger influence on the buildings' energy performance in the highest range of the thermal transmittance scale. In contrast, the lowest range of U -values tends to be very similar among timeframes.

When analyzing the impact of using present-day ideal U -values in future buildings, Table 12 shows that the energy demand difference is equal to or smaller than 2 % in 2050. For example, Caxias do Sul shows an energy difference of $0.1 \text{ MW}\cdot\text{h} \pm 0.03 \text{ MW}\cdot\text{h}$ (2 %) from having less $0.15 \text{ W}\cdot\text{m}^{-2}\cdot\text{K}^{-1}$ in opaque elements and $0.6 \text{ W}\cdot\text{m}^{-2}\cdot\text{K}^{-1}$ in transparent elements. Compared to the ideal U -values from 2080, however, the energy differences are higher, reaching 5 % in Santa Maria ($0.41 \text{ MW}\cdot\text{h} \pm 0.04 \text{ MW}\cdot\text{h}$) and Porto Alegre ($0.42 \text{ MW}\cdot\text{h} \pm 0.04 \text{ MW}\cdot\text{h}$)—having more $0.5 \text{ W}\cdot\text{m}^{-2}\cdot\text{K}^{-1}$ and $0.45 \text{ W}\cdot\text{m}^{-2}\cdot\text{K}^{-1}$ for the opaque elements, respectively, and $2 \text{ W}\cdot\text{m}^{-2}\cdot\text{K}^{-1}$ and $1.8 \text{ W}\cdot\text{m}^{-2}\cdot\text{K}^{-1}$ for the transparent elements, respectively.

Table 12

Group 4 – Overheating from the present-day ideal U -values in future timeframes (impacts greater or equal to 3% are marked in bold).

Location	Present-day ideal U -values	2050				2080			
		Ideal U -values	Impact of present-day ideal U -values		Ideal U -values	Impact of present-day ideal U -values			
			Energy (MW-h)	Δ energy (MW-h)		Δ energy (%)	ΔU -values* ($W\cdot m^{-2}\cdot K^{-1}$)	Energy (MW-h)	Δ energy (MW-h)
Poços de Caldas (> 900 m)	0.90/3.6	5.54 ± 0.50	0.05 ± 0.03	1	−0.05/−0.2	7.85 ± 0.70	0.24 ± 0.04	3	−0.45/−1.8
Curitiba (> 900 m)	1.20/4.8	3.91 ± 0.38	0.01 ± 0.02	< 1	+0.05/+0.2	6.61 ± 0.59	0.04 ± 0.04	1	−0.05/−0.2
Passo Fundo (> 700 m)	0.80/3.2	5.11 ± 0.43	0.04 ± 0.03	1	+0.05/+0.2	7.36 ± 0.65	0.01 ± 0.04	< 1	−0.05/−0.2
Caxias do Sul (> 700 m)	0.80/3.2	4.73 ± 0.47	0.10 ± 0.03	2	+0.15/+0.6	7.00 ± 0.67	0.06 ± 0.04	1	−0.05/−0.2
Santa Maria (sea level)	0.65/2.6	6.49 ± 0.54	0.04 ± 0.04	1	−0.20/−0.8	8.70 ± 0.73	0.41 ± 0.04	5	−0.50/−2.0
Porto Alegre (coastal)	0.70/2.8	6.54 ± 0.56	0 ± 0.04	–	–	8.92 ± 0.74	0.42 ± 0.04	5	−0.45/−1.8
Pelotas (coastal)	0.75/3.0	5.42 ± 0.48	0.06 ± 0.03	1	+0.10/+0.4	7.83 ± 0.66	0.03 ± 0.05	< 1	+0.10/+0.4

* Opaque and transparent elements' delta U -values, respectively, for the difference between present-day and future ideal U -values.

4. Discussion and conclusions

The results show that the ideal thermal transmittances of the residential building's envelope vary in different regions of Brazil. As the outdoor environment warms due to climate change, these values will shift dramatically in several locations.

These findings have significant consequences, implying radically new design strategies to mitigate climate change. For example, Group 1 shows that, in today's climate and future timeframes, the ideal U -values must be the lowest possible (Table 13 summarizes the trend of ideal U -values per group). Therefore, the design strategy is straightforward in this group, constrained by other factors, such as cost and availability of resources. As the outdoor dry-bulb temperatures are so high, even for the present-day climate—minimum temperatures vary between 21 °C and 25 °C in this group's locations (Table 14 summarizes the outdoor dry-bulb air temperatures per group and climate)—buildings must prevent any heat transfer from the outside. In this group, night ventilation has small benefits in present-day and future climates.

However, this strategy does not work in Group 2 and Group 3. Although the lowest thermal transmittances possible in future timeframes are recommended, the ideal U -values must be the highest possible in the present-day climate. This shift is dramatic and means that small environmental changes will greatly impact the energy performance of buildings. For instance, when compared to the present buildings with high ideal U -values, thermal energy needs may reach 30 % more in 2050 and 57 % in 2080 in Group 2 and 25 % more in 2080 in Group 3. Therefore, in this case, the design strategy should consider using the highest thermal transmittances in today's buildings and retrofitting them as the climate evolves (Table 13). This strategy will be easier to implement in Group 3 but rather difficult in Group 2, as the shift from highest to lowest thermal transmittances is expected to occur in the next two decades (2050 timeframe). The difference in Group 3 is due to slightly lower temperatures of locations in higher altitudes

Table 13

Summary of the ideal U -values trend.

	Present day	SSP5–8.5	
		2050	2080
Group 1	Lowest	Lowest	Lowest
Group 2	Highest	Lowest	Lowest
Group 3	Highest	Highest	Lowest
Group 4	High to Mid		Mid to Low

Table 14

Summary of present-day and future climate average outdoor dry-bulb air temperatures and averages of daily minimum and maximum dry-bulb air temperatures.

	Latitudes	Present-day climate			SSP5–8.5	
		Min.	Avg.	Max.	Min. 2050	Min. 2080
Group 1	3° S to 17° S	21 °C to 25 °C	25 °C to 29 °C	29 °C to 35 °C	24 °C to 28 °C	27 °C to 30 °C
Group 2	16° S to 24° S	17 °C to 22 °C	22 °C to 24 °C	27 °C to 31 °C	20 °C to 24 °C	23 °C to 27 °C
Group 3	14° S to 24° S	17 °C to 18 °C	20 °C to 22 °C	25 °C to 28 °C	19 °C to 21 °C	22 °C to 24 °C
Group 4	21° S to 32° S	9 °C to 14 °C	17 °C to 19 °C	22 °C to 27 °C	12 °C to 17 °C	15 °C to 20 °C

(Table 14).

Group 4 has two main trends for ideal U -values (Table 13); therefore, different design strategies are needed. Following the trend to have lower temperatures as the latitude descends, this group shows the average daily minimum dry-bulb air temperatures clearly below the heating setpoint for present-day and future climates (Table 14), thus having some heating needs for higher thermal transmittance values. In some locations, the trend is to have lower U -values in the future, such as in Poços de Caldas, Santa Maria, and Porto Alegre. In these cases, the design strategy might be to design buildings optimized for today's climate. However, buildings will need to be retrofitted in the future—for instance, in Porto Alegre, in 2080, an addition of 10 cm of insulation in the building walls (increase from 4 cm to 14 cm) will be required for the same single-family house with a common double-brick wall construction to reduce its U -value in 0.45 $W\cdot m^{-2}\cdot K^{-1}$, and thus reach the future ideal value. Alternatively, the design strategy might already consider lower values in the present, but buildings will underperform before the climate gets warmer enough to become optimal. In this latter case, the risk associated with how the climate will evolve is assumed in the building design today. In Curitiba, Passo Fundo, Caxias do Sul, and Pelotas, the ideal U -values are close to those for the future climate. In these cases, building design can easily accommodate the evolving climate and find a balanced design, particularly as the energy demand differences are below 1 % in 2080.

In all cases where future changes in thermal transmittance are required (Groups 2, 3, and 4), the tendency is to increase the thermal resistance, which usually involves adding insulation layers to the

building fabric. Although implying structural modifications, this process is relatively straightforward compared to other world regions, where the results point to an opposite trend, requiring less insulation [7,13].

Even if heating needs are observed in some southern locations, the thermal energy demand is minimal compared to the cooling requirements when ideal thermal transmittance values are considered. Thus, no significant alterations are expected in the future of total cooling-dominated needs. However, in the current poorly insulated dwellings of southern Brazil, which have significant heating needs, substantial changes will be imposed by the climate change toward fully cooling habits.

This study has some associated uncertainties and limitations that need to be discussed. Relatively to uncertainties, these are related to the validity of the climate model data, the representativeness of the climate model grid and the present-day weather to be morphed, and the morphing procedure itself. Relatively to limitations, first, the functional program and the operation specifications do not capture all the different characteristics of single-family houses found in Brazil. Second, although the study covers many locations, these in no way cover all the locations, some for lack of weather data and others for the lack of typical meteorological year files derived from records from the baseline period. Third, this study only analyzed the SSP5–8.5 scenario, which might provide an incomplete perspective of the impacts of climate change since there are other scenarios. These scenarios may prove more probable if the countries' carbon emissions and other greenhouse gases are reduced. Lastly, projections from different climate models may diverge significantly. In this sense, this study only provides a snapshot of what might be probable, as it only used data from EC-Earth3.

This study's findings have several implications. First, although climate change increases the outdoor dry-bulb air temperatures equally throughout Brazil, the impact on the buildings' ideal U -values varies depending on each region, thus showing the need for local policies and specific building design strategies. These design strategies might change dramatically in some regions, particularly when the average outdoor dry-bulb air temperature and average daily minimum dry-bulb air temperature fall below the heating setpoint, between the heating and cooling setpoints (20 °C and 25 °C, respectively), and the average outdoor dry-bulb air temperature is higher than the cooling setpoint. As summarized in Table 15, it is possible to roughly determine the ideal U -values from the relationship between the average daily minimum and dry-bulb temperatures and the building's heating and cooling setpoints. Therefore, according to this relationship, it is possible to rapidly predict the trend of ideal U -values by determining how the relationship varies over time. For example, when the relationship changes over time, the buildings' ideal U -values will tend to increase or decrease and, in some cases, may even be drastically different. Table 16 lists the possible trends and proposes design strategies accordingly. In order to implement an effective design strategy, professionals should consider how climate evolves over the life span of the building. This may be particularly difficult since there are several potential scenarios, some more likely

Table 15

Ideal U -values range and their relationship with the outdoor dry-bulb temperatures (average daily minimum dry-bulb temperature and average dry-bulb temperature).

ID	Ideal U -values range	Avg. daily minimum temperature	Avg. dry-bulb temperature
A	Mid-range	Lower than the heating setpoint	Lower than the heating setpoint
B	Highest range	Lower than the heating setpoint	Higher than the heating setpoint and lower than the cooling setpoint
C	Any value	Similar or higher than the heating setpoint	Similar or lower than the cooling setpoint
D	Lowest range	Higher than the heating setpoint	Higher than the cooling setpoint

Table 16

Proposed design strategy according to each possible trend of ideal U -values. As the climate becomes warmer in the future, the trend is only upward in the letters (*i.e.*, we assume that a trend will never be from D to C or B to A).

Trend	Proposed design strategy
No change	Optimize thermal transmittance for today's climate.
A to B	In this case, the trend is to have higher U -values in the future. In order to prevent downgrading the building to a lower insulation level in the future, it is recommended that professionals consider a balanced approach that includes both present-day and future climates. The building will underperform in any specific climate timeframe but will be the best considering the life span of the building.
A/B to C	In these cases, as the thermal performance will be similar over the whole range of the thermal transmittance in the future, the building should be designed for the present-day climate.
A/B to D	This change is the most dramatic. In this case, buildings should be designed for present-day climate and retrofitted over time. Therefore, the adopted construction technology must facilitate future retrofits. This approach is conservative and minimizes assuming the risk of designing a building for a future scenario that may not occur. This strategy is ideal as the building will be optimal over time.
C to D	In this case, as the thermal performance is similar over the whole range of the thermal transmittance in present-day climate, the building should be designed for a future climate scenario.

than others.

These findings also open a new question, particularly related to the impact of the urban heat island effect. One may wonder if such findings can be observed in today's cities and question the combined impact of climate change and urban heat island effect in colder climates of Brazil (particularly in Group 4). If such findings are observed in an urban context, different building design strategies are needed for rural and urban areas.

As future research, the body of knowledge would benefit from studying other climate scenarios, other building types, design characteristics—*i.e.*, alternative roof type, shading elements, alternative internal gains and ventilation strategies—, and the combined impact of climate change and urban heat island effect. From a methodological perspective, the robustness of results would benefit from using an ensemble of climate models to reduce a model-specific bias.

The main conclusions from this study are the following:

- Although the relative increase in outdoor air temperatures is equal throughout Brazil, the impact on the buildings' ideal U -values over time may lead to dramatic changes depending on the region.
- Low thermal transmittance values increase robustness to climate change—*i.e.*, the rise in energy demand resulting from climate change is smaller when buildings have low U -values. However, this does not mean that low U -values are beneficial. For instance, in Groups 2, 3, and 4, very low U -values have greater energy demand than higher U -values in the present-day climate—this higher demand is even observed for Groups 3 and 4 in the 2050 and 2080 timeframes.
- Where the ideal U -values are in the thermal transmittance scale, it also corresponds to the lowest building geometry influence. This relation occurs in any climate, be it in the present day or future timeframe. In Group 1, it occurs in the lowest part of the U -values scale for all timeframes; in Group 2, it is in the highest part of the U -values scale for the present-day climate; in Group 3, it is found in the highest part of the U -values scale for the present-day and 2050 climate; and finally, in Group 4, it is generally in the middle of the U -values scale where the ideal U -values are found. This means the buildings' energy performances with other U -values tend to diverge, making their shape and glazing areas more relevant. This is true for both low and high thermal transmittances.
- When the average daily minimum dry-bulb air temperature (> 20 °C) and the average dry-bulb temperatures (< 25 °C) are within the

setpoints of the HVAC system (20 °C for heating and 25 °C for cooling), the energy demand of buildings gets similar over the thermal transmittance scale; thus, the energy differences between ideal U -values and other values become less relevant. This effect is found for (i) Goiânia (Group 1), Macaé, and Rio de Janeiro (Group 2) in the present-day climate, (ii) Santos, Maringá (Group 2), Franca, and São Carlos (Group 3) in 2050, and (iii) São Paulo (Group 3) in 2080.

- The building design strategies will change dramatically when the evolving climate warms enough to shift through the relationship stated in the previous item. This shift goes from having buildings with their minimum energy demand in the highest range of U -values to having their ideal U -values in the lowest range. This conclusion and the diversity of ideal U -values over Brazil implies implementing regional building energy policies and professionals finding new design strategies to address climate change.

CRedit authorship contribution statement

Eugénio Rodrigues: Writing – review & editing, Writing – original draft, Visualization, Supervision, Software, Project administration, Methodology, Investigation, Funding acquisition, Formal analysis, Data curation, Conceptualization. **Jean Parente:** Writing – review & editing, Writing – original draft, Investigation. **Marco S. Fernandes:** Writing – review & editing, Software, Investigation, Conceptualization.

Declaration of Competing Interest

The authors declare that they have no known competing financial interests or personal relationships that could have appeared to influence the work reported in this paper.

Data availability

The dataset of the experiment is available at the URL: <https://doi.org/10.6084/m9.figshare.23932626>.

Acknowledgments

The presented work is framed under the *Energy for Sustainability Initiative* of the University of Coimbra (UC).

We acknowledge the World Climate Research Programme, which, through its Working Group on Coupled Modeling, coordinated and promoted CMIP6. In addition, we thank the climate modeling groups for producing and making available their model output, the Earth System Grid Federation (ESGF) for archiving the data and providing access, and the multiple funding agencies that support CMIP6 and ESGF.

The Portuguese Foundation for Science and Technology (FCT) supported this work [grant number PTDC/EME-REN/3460/2021 and doi:10.54499/PTDC/EME-REN/3460/2021]. In addition, FCT supports Eugénio Rodrigues and Marco S. Fernandes through researcher contracts [2021.00230.CEECIND and 2021.02975.CEECIND, respectively].

References

- [1] United Nations Environment Programme. Towards a zero-emissions, efficient and resilient buildings and construction sector. 2019 Global Status report. 2019.
- [2] Rosenzweig C, Karoly D, Vicarelli M, Neofotis P, Wu Q, Casassa G, et al. Attributing physical and biological impacts to anthropogenic climate change. *Nature* 2008; 453:353–7. <https://doi.org/10.1038/nature06937>.
- [3] Khraishah H, Alahmad B, Ostergard RL, AlAshqar A, Albaghdadi M, Vellanki N, et al. Climate change and cardiovascular disease: implications for global health. *Nat Rev Cardiol* 2022. <https://doi.org/10.1038/s41569-022-00720-x>.
- [4] Cabeza LF, Châfer M. Technological options and strategies towards zero energy buildings contributing to climate change mitigation: a systematic review. *Energy Buildings* 2020;219:110009. <https://doi.org/10.1016/j.enbuild.2020.110009>.
- [5] Bamdad K, Cholette ME, Omrani S, Bell J. Future energy-optimised buildings — addressing the impact of climate change on buildings. *Energy Buildings* 2021;231: 110610. <https://doi.org/10.1016/j.enbuild.2020.110610>.
- [6] Urge-Vorsatz D, Petrichenko K, Staniec M, Eom J. Energy use in buildings in a long-term perspective. *Curr Opin Environ Sustain* 2013;5:141–51. <https://doi.org/10.1016/j.cosust.2013.05.004>.
- [7] Rodrigues E, Fernandes MS. Overheating risk in Mediterranean residential buildings: Comparison of current and future climate scenarios. *Appl Energy* 2020; 259:114110. <https://doi.org/10.1016/j.apenergy.2019.114110>.
- [8] De Masi RF, Gigante A, Ruggiero S, Vanoli GP. Impact of weather data and climate change projections in the refurbishment design of residential buildings in cooling dominated climate. *Appl Energy* 2021;303:117584. <https://doi.org/10.1016/j.apenergy.2021.117584>.
- [9] Ascione F, De Masi RF, Gigante A, Vanoli GP. Resilience to the climate change of nearly zero energy-building designed according to the EPBD recast: monitoring, calibrated energy models and perspective simulations of a Mediterranean nZEB living lab. *Energy Buildings* 2022;262:112004. <https://doi.org/10.1016/j.enbuild.2022.112004>.
- [10] Walker L, Hischer I, Schlueter A. Does context matter? Robust building retrofit decision-making for decarbonization across Europe. *Build Environ* 2022;226: 109666. <https://doi.org/10.1016/j.buildenv.2022.109666>.
- [11] Pajek L, Jevrić M, Čipranić I, Košir M. A multi-aspect approach to energy retrofitting under global warming: a case of a multi-apartment building in Montenegro. *J Build Eng* 2023;63:105462. <https://doi.org/10.1016/j.jobe.2022.105462>.
- [12] Zou Y, Xiang K, Zhan Q, Li Z. A simulation-based method to predict the life cycle energy performance of residential buildings in different climate zones of China. *Build Environ* 2021;193:107663. <https://doi.org/10.1016/j.buildenv.2021.107663>.
- [13] Rodrigues E, Azimi Fereidani N, Fernandes MS, Gaspar AR. Climate change and ideal thermal transmittance of residential buildings in Iran. *J Build Eng* 2023;74: 106919. <https://doi.org/10.1016/j.jobe.2023.106919>.
- [14] Shen P, Brahm W, Yi Y. The feasibility and importance of considering climate change impacts in building retrofit analysis. *Appl Energy* 2019;233–234:254–70. <https://doi.org/10.1016/j.apenergy.2018.10.041>.
- [15] Verichev K, Zamorano M, Fuentes-Sepúlveda A, Cárdenas N, Carpio M. Adaptation and mitigation to climate change of envelope wall thermal insulation of residential buildings in a temperate oceanic climate. *Energy Buildings* 2021;235:110719. <https://doi.org/10.1016/j.enbuild.2021.110719>.
- [16] Dalbem R, Grala da Cunha E, Vicente R, Figueiredo A, Oliveira R, da Silva ACSB. Optimisation of a social housing for south of Brazil: from basic performance standard to passive house concept. *Energy* 2019;167:1278–96. <https://doi.org/10.1016/j.energy.2018.11.053>.
- [17] Vettorazzi E, Figueiredo A, Rebelo F, Vicente R, Grala da Cunha E. Optimization of the passive house concept for residential buildings in the South-Brazilian region. *Energy Buildings* 2021;240:110871. <https://doi.org/10.1016/j.enbuild.2021.110871>.
- [18] Benincá L, Crespo Sánchez E, Passuello A, Karini Leitzke R, Grala da Cunha E, Barroso Maria González, et al. Multi-objective optimization of the solar orientation of two residential multifamily buildings in South Brazil. *Energy Buildings* 2023;285: 112838. <https://doi.org/10.1016/j.enbuild.2023.112838>.
- [19] Nunes G, Giglio T. Effects of climate change in the thermal and energy performance of low-income housing in Brazil—assessing design variable sensitivity over the 21st century. *Renew Sustain Energy Rev* 2022;168:112885. <https://doi.org/10.1016/j.rser.2022.112885>.
- [20] Invidiata A, Ghisi E. Impact of climate change on heating and cooling energy demand in houses in Brazil. *Energy Buildings* 2016;130:20–32. <https://doi.org/10.1016/j.enbuild.2016.07.067>.
- [21] Triana MA, Lamberts R, Sassi P. Should we consider climate change for Brazilian social housing? Assessment of energy efficiency adaptation measures. *Energy Buildings* 2018;158:1379–92. <https://doi.org/10.1016/j.enbuild.2017.11.003>.
- [22] Triana MA, Lamberts R, Sassi P. Sustainable energy performance in Brazilian social housing: a proposal for a Sustainability Index in the energy life cycle considering climate change. *Energy Buildings* 2021;242:110845. <https://doi.org/10.1016/j.enbuild.2021.110845>.
- [23] da Guarda ELA, Domingos RMA, Gabriel E, Durante LC, Moreira JVR, Sanches JCM. Use of thermal insulation in the envelope to mitigate energy consumption in the face of climate change for mid-western Brazil. *IOP Conf Ser Earth Environ Sci* 2020;410:012009. <https://doi.org/10.1088/1755-1315/410/1/012009>.
- [24] Cruz AS, da Cunha EG. The impact of climate change on the thermal-energy performance of the SCIP and ICF wall systems for social housing in Brazil. *Indoor Built Environ* 2022;31:838–52. <https://doi.org/10.1177/1420326X211038047>.
- [25] Beck HE, Zimmermann NE, McVicar TR, Vergopolan N, Berg A, Wood EF. Present and future Köppen-Geiger climate classification maps at 1-km resolution. *Sci Data* 2018;5:180214. <https://doi.org/10.6084/m9.figshare.6396959>.
- [26] Climate.OneBuilding.Org. Repository of free climate data for building performance simulation. <http://climate.onebuilding.org/default.html>; 2021 (accessed May 27, 2021).
- [27] Belcher S, Hacker J, Powell D. Constructing design weather data for future climates. *Build Serv Eng Res Technol* 2005;26:49–61. <https://doi.org/10.1191/0143624405bt1120a>.
- [28] Rodrigues E, Carvalho D, Fernandes MS. Future Weather Generator – Morphs current weather for performance simulation of buildings in the future. <http://adaa.pt/future-weather-generator/>; 2022.
- [29] Eyring V, Bony S, Meehl GA, Senior CA, Stevens B, Stouffer RJ, et al. Overview of the Coupled Model Intercomparison Project Phase 6 (CMIP6) experimental design and organization. *Geosci Model Dev* 2016;9:1937–58. <https://doi.org/10.5194/gmd-9-1937-2016>.

- [30] Hazeleger W, Wang X, Severijns C, Ștefănescu S, Bintanja R, Sterl A, et al. EC-Earth V2.2: description and validation of a new seamless earth system prediction model. *Climate Dynam* 2012;39:2611–29. <https://doi.org/10.1007/s00382-011-1228-5>.
- [31] Haarsma R, Acosta M, Bakhshi R, Bretonnière P-A, Caron L-P, Castrillo M, et al. HighResMIP versions of EC-Earth: EC-Earth3P and EC-Earth3P-HR – description, model computational performance and basic validation. *Geosci Model Dev* 2020;13:3507–27. <https://doi.org/10.5194/gmd-13-3507-2020>.
- [32] Lee J-Y, Marotzke J, Bala G, Cao L, Corti S, Dunne JP, et al. Future global climate: scenario-based projections and near-term information. *Clim. Chang.* 2021 Phys. Sci. Basis. Contrib. Work. Gr. I to Sixth Assess. Rep. Intergov. Panel Clim. Chang. Cambridge, UK and New York, NY, USA: Cambridge University Press; 2021. p. 553–672. <https://doi.org/10.1017/9781009157896.006>.
- [33] Hausfather Z, Peters GP. Emissions – the ‘business as usual’ story is misleading. *Nature* 2020;577:618–20. <https://doi.org/10.1038/d41586-020-00177-3>.
- [34] O’Neill BC, Tebaldi C, van Vuuren DP, Eyring V, Friedlingstein P, Hurtt G, et al. The Scenario Model Intercomparison Project (ScenarioMIP) for CMIP6. *Geosci Model Dev* 2016;9:3461–82. <https://doi.org/10.5194/gmd-9-3461-2016>.
- [35] Rodrigues E, Fernandes MS, Carvalho D, Fernandes MS. Documentation of Future Weather Generator. <https://adai.pt/future-weather-generator/documentation/>; 2022.
- [36] Rodrigues E, Fernandes MS, Gomes Á, Gaspar AR, Costa JJ. Performance-based design of multi-story buildings for a sustainable urban environment: a case study. *Renew Sustain Energy Rev* 2019;113:109243. <https://doi.org/10.1016/j.rser.2019.109243>.
- [37] Rodrigues E, Gaspar AR, Gomes Á. An evolutionary strategy enhanced with a local search technique for the space allocation problem in architecture, Part 1: Methodology. *Comput Des* 2013;45:887–97. <https://doi.org/10.1016/j.cad.2013.01.001>.
- [38] Rodrigues E, Gaspar AR, Gomes Á. An approach to the multi-level space allocation problem in architecture using a hybrid evolutionary technique. *Autom Constr* 2013;35:482–98. <https://doi.org/10.1016/j.autcon.2013.06.005>.
- [39] Rodrigues E, Gaspar AR, Gomes Á. An evolutionary strategy enhanced with a local search technique for the space allocation problem in architecture, Part 2: Validation and performance tests. *Comput Des* 2013;45:898–910. <https://doi.org/10.1016/j.cad.2013.01.003>.
- [40] Rodrigues E, Gaspar AR, Gomes Á. Automated approach for design generation and thermal assessment of alternative floor plans. *Energy Buildings* 2014;81:170–81. <https://doi.org/10.1016/j.enbuild.2014.06.016>.
- [41] Passivhaus Institut. <https://passiv.de>; 2015 (accessed November 23, 2022).
- [42] Dai HK, Chen C. Air infiltration rates in residential units of a public housing estate in Hong Kong. *Build Environ* 2022;219:109211. <https://doi.org/10.1016/j.buildenv.2022.109211>.
- [43] Miszczuk A, Heim D. Parametric study of air infiltration in residential buildings—the effect of local conditions on energy demand. *Energies* 2020;14:127. <https://doi.org/10.3390/en14010127>.